Molecular Therapy
Original Article

mRNA-LNP vaccine-induced CD8+ T cells protect mice from lethal SARS-CoV-2 infection in the absence of specific antibodies

Brian Montoya,[1] Carolina R. Melo-Silva,[1] Lingjuan Tang,[1] Samita Kafle,[1] Peter Lidskiy,[2] Csaba Bajusz,[3,4] Máté Vadovics,[3] Hiromi Muramatsu,[3] Edit Abraham,[4,5] Zoltan Lipinszki,[4,5] Debotri Chatterjee,[6] Gabrielle Scher,[1] Juliana Benitez,[1] Molly M.H. Sung,[7] Ying K. Tam,[7] Nicholas J. Catanzaro,[8] Alexandra Schäfer,[8] Raul Andino,[2] Ralph S. Baric,[8] David R. Martinez,[9] Norbert Pardi,[3] and Luis J. Sigal[1]

[1]Department of Microbiology and Immunology, Bluemle Life Science Building, Thomas Jefferson University, Philadelphia, PA 19107, USA; [2]Department of Microbiology and Immunology, University of California, San Francisco, San Francisco, CA 94158, USA; [3]Department of Microbiology, Perelman School of Medicine, University of Pennsylvania, Philadelphia, PA 19104, USA; [4]National Laboratory for Biotechnology, Institute of Genetics, HUN-REN Biological Research Centre, Szeged, Hungary; [5]MTA SZBK Lendület Laboratory of Cell Cycle Regulation, Synthetic and Systems Biology Unit, Institute of Biochemistry, HUN-REN Biological Research Centre, Szeged, Hungary; [6]Department of Neurosciences, Thomas Jefferson University Vickie and Jack Farber Institute for Neuroscience, Philadelphia, PA, USA; [7]Acuitas Therapeutics, Vancouver, BC V6T 1Z3, Canada; [8]Department of Epidemiology, Microbiology and Immunology, University of North Carolina at Chapel Hill, Chapel Hill, NC 27599, USA; [9]Department of Immunobiology, Center for Infection and Immunity, Yale School of Medicine, New Haven, CT 06520, USA

The role of CD8+ T cells in SARS-CoV-2 pathogenesis or mRNA-LNP vaccine-induced protection from lethal COVID-19 is unclear. Using mouse-adapted SARS-CoV-2 virus (MA30) in C57BL/6 mice, we show that CD8+ T cells are unnecessary for the intrinsic resistance of female or the susceptibility of male mice to lethal SARS-CoV-2 infection. Also, mice immunized with a di-proline prefusion-stabilized full-length SARS-CoV-2 Spike (S-2P) mRNA-LNP vaccine, which induces Spike-specific antibodies and CD8+ T cells specific for the Spike-derived VNFNFNGL peptide, are protected from SARS-CoV-2 infection-induced lethality and weight loss, while mice vaccinated with mRNA-LNPs encoding only VNFNFNGL are protected from lethality but not weight loss. CD8+ T cell depletion ablates protection in VNFNFNGL but not in S-2P mRNA-LNP-vaccinated mice. Therefore, mRNA-LNP vaccine-induced CD8+ T cells are dispensable when protective antibodies are present but essential for survival in their absence. Hence, vaccine-induced CD8+ T cells may be critical to protect against SARS-CoV-2 variants that mutate epitopes targeted by protective antibodies.

INTRODUCTION

Virus-infected cells degrade viral proteins in their cytosol. Some of the resulting eight to nine amino-acid-long peptides bind to major histocompatibility complex class I (MHC class I) molecules and are displayed at the cell surface.[1] When CD8+ T cells recognize MHCI-I peptide complexes at the surface of professional antigen-presenting cells through their specific T cell receptor (TCR), they proliferate and differentiate into effectors that can kill any infected cell that displays the cognate peptide with MHC class I. If the infection is controlled, ~90% of the antigen-specific effector CD8+ T cells die. Those that remain differentiate into antigen-specific memory CD8+ T cells (mCD8+) that can rapidly become effectors following reinfection and may contribute to a more effective virus control and disease prevention.[2–4] Notably, effector CD8+ T cells can be double-edged swords. By rapidly killing infected cells, they play a major role in pathogen clearance and intrinsic or acquired resistance to some viral diseases. However, in other cases, the killing of infected cells and the ensuing inflammation they induce can result in immunopathology.[2,4–13] The role of CD8+ T cells in intrinsic or acquired susceptibility or resistance to SARS-CoV-2 needs to be better understood.

Vaccines safely mimic infections to induce immune responses that confer protection against pathogens. Vaccines exploit the adaptive immune system's ability to recognize and respond to antigens produced by pathogens to resolve subsequent infections more rapidly than in naive hosts.[14] Traditionally, vaccines have been created using the entire killed or attenuated pathogen or subunits of the pathogen that induce protective immune responses.[14] More recently, messenger RNA (mRNA) vaccines emerged as a novel modality that proved to be effective against pathogens such as severe acute respiratory syndrome coronavirus 2 (SARS-CoV-2), the causative agent of coronavirus disease 2019 (COVID-19).[15] Critical discoveries, such as the incorporation of

Received 12 September 2023; accepted 8 April 2024;
https://doi.org/10.1016/j.ymthe.2024.04.019.

Correspondence: Norbert Pardi, Department of Microbiology, Perelman School of Medicine, University of Pennsylvania, Philadelphia, PA 19104, USA.
E-mail: pnorbert@pennmedicine.upenn.edu
Correspondence: Luis J. Sigal, Department of Microbiology and Immunology, Bluemle Life Science Building, Thomas Jefferson University, Philadelphia, PA 19107, USA.
E-mail: luis.sigal@jefferson.edu

Please cite this article in press as: Montoya et al., mRNA-LNP vaccine-induced CD8+ T cells protect mice from lethal SARS-CoV-2 infection in the absence of specific antibodies, Molecular Therapy (2024), https://doi.org/10.1016/j.ymthe.2024.04.019

modified nucleosides into the mRNA to reduce innate immune recognition, improved mRNA purification techniques, and encapsulation of the mRNA into ionizable lipid-containing lipid nanoparticles (LNPs), significantly contributed to the development of this potent vaccine platform against infectious diseases.[16–21] Nucleoside-modified mRNA-LNP vaccines developed by Moderna and Pfizer-BioNTech (BNT) are used around the world to vaccinate against SARS-CoV-2 and have substantially altered the course of the pandemic, saving millions of lives globally.[22] These SARS-CoV-2 vaccines target the Spike (S) surface glycoprotein, which mediates viral cell entry by binding to the angiotensin-converting enzyme 2 (ACE2).[23,24] The S protein has two subunits: S1, which contains the receptor binding domain (RBD), and S2, responsible for viral fusion with the host cell membrane.[25] The initial Moderna and Pfizer-BioNTech COVID-19 mRNA vaccines contained Spike from the ancestral SARS-CoV-2 Wuhan-1 strain (Wuhan-1) modified with K986P and V987P substitutions to stabilize S in the prefusion conformation. This modified Spike, known as S-2P (Figure S1), is thought to induce superior neutralizing antibody (nAb) responses compared with a non-prefusion-stabilized wild-type S.[15,26]

Most studies of SARS-CoV-2 mRNA-LNP vaccines correlate protection with the presence of anti-S, anti-RBD, or nAbs in sera.[27–30] However, mouse and nonhuman primate studies and human data show that, in addition to Abs, nucleoside-modified mRNA-LNP SARS-CoV-2 vaccines induce strong CD8+ T cell responses.[31–34] Depletion of these virus-specific CD8+ T cells resulted in higher viral burden in the lungs of vaccinated animals, suggesting a role in protection against COVID-19.[35,36]

We have shown previously that mCD8+ T cells, including those induced by mRNA-LNP vaccines, can protect mice from ectromelia virus infection.[11,12,34,37–39] Others have found that, at 21 days post-boost (dpb), mice immunized with the Pfizer-BioNTech BNT162b2 mRNA-LNP vaccine have an expanded population of CD8+ T cells specific for the highly conserved and immunodominant SARS-CoV-1 and SARS-CoV-2 Spike protein-derived epitope VNFNFNGL bound to the MHC class I molecule K^b.[31,40–47] However, it is unknown whether these CD8+ T cells play a role in protection from SARS-CoV-2 infection or severe disease in a mouse model that recapitulates the acute lung injury observed in human SARS-CoV-2 infections.

The Spike of the Wuhan-1 virus binds human but not mouse ACE2. Thus, mice are not susceptible to infection with Wuhan-1. However, K18- hACE2 transgenic mice in the C57BL/6 (B6) background expressing the human ACE2 (hACE2) receptor driven by the human cytokeratin 18 (K18) promoter are susceptible to Wuhan-1 infection.[48,49] In addition, Wuhan-1 adapted to mice by genetic engineering of Spike followed by 30 passages in BALB/c mice (MA30) recapitulates SARS-CoV-2 human infection in young BALB/c and middle-aged B6 mice.[50] MA30's Spike differs from Wuhan-1's in only five amino acids (Figure S1).

We now show that, similar to human infection with Wuhan-1, MA30 is more pathogenic to male than to female B6 mice and that neither the intrinsic resistance of females nor the susceptibility of males requires CD8+ T cells. We further show that male B6 and female K18-hACE2 mice immunized with nucleoside-modified S-2P mRNA-LNPs, which have Abs in serum and K^b-VNFNFNGL-specific CD8+ T cells in peripheral blood, do not display signs of disease following infection of B6 mice with MA30 or K18-hACE2 mice with Wuhan-1 SARS-CoV-2 whether depleted or not of CD8+ T cells. This indicates that, in the presence of Abs, mCD8+ T cells are unnecessary for protection from SARS-CoV-2-induced disease or lethality. On the other hand, B6 male and female K18- hACE2 mice immunized with LNPs loaded with a mini-mRNA encoding only for VNFNFNGL, which lack Abs but have high frequencies of K^b-VNFNFNGL-specific CD8+ T cells, endure some weight loss but are protected from lethality. This demonstrates that CD8+ T cells specific for an immunodominant SARS-CoV-2 CD8+ T cell epitope induced by mRNA-LNP vaccination can reduce viral load and protect mice from SARS-CoV-2 lethality.

RESULTS

CD8+ T cells are not required for intrinsic resistance or susceptibility to COVID-19-like disease in mice

CD8+ T cells are critical for intrinsic resistance to some viral diseases. Still, they can also induce pathology during infection by a variety of viruses, such as hepatitis B virus, respiratory syncytial virus, lymphocytic choriomeningitis virus , and influenza A virus.[8–10,51] Thus, we sought to determine whether CD8+ T cells are involved in the pathogenesis of SARS-CoV-2 infection in mice. In initial experiments, we found that all mid-aged (90–230 days old) female B6 mice survived intranasal infection (Figure 1A) with 50,000 plaque-forming units (pfu) SARS-CoV-2 MA30 with transient, weight loss (Figure 1B). Conversely, ∼50% of mid-aged males succumbed to the infection (Figure 1A), and the survivors experienced prolonged weight loss (Figure 1B). The difference in sex susceptibility of mid-aged B6 mice to MA30 was akin to the findings by Davis et al. with the independently made SARS-CoV-2 MA10 strain.[52]

Depletion of CD8+ T cell with 100 μg mAb 2.43 (Figure S2) did not affect the respective susceptibility or resistance of mid-aged male and female mice to MA30 Figures 1C–1F). These data indicate that CD8+ T cells are not required for the respective intrinsic resistance or susceptibility of mid-aged B6 female or male mice to MA30 infection.

The prime-boost interval does not affect the CD8+ T cell or antibody responses after immunization with 10 μg S-2P mRNA-LNP in B6 mice

To analyze the role of CD8+ T cells in mRNA-LNP vaccine-mediated protection from lethal SARS-CoV-2 infection, we first optimized the immunization regime of the S-2P mRNA-LNP vaccine. The initial Moderna and Pfizer-BioNTech S-2P mRNA-LNP SARS-CoV-2 vaccine regimen in humans was two intramuscular (i.m.) inoculations, prime and boost, ∼30–60 days apart. Later, additional boosts were added with an increased interval.[53,54] We have shown previously that a prime-boost interval of 2 weeks with an mRNA-LNP vaccine administered intradermally (i.d.) induced fully protective CD8+ T cells against ectromelia virus infection in susceptible mice.[34] This

Please cite this article in press as: Montoya et al., mRNA-LNP vaccine-induced CD8+ T cells protect mice from lethal SARS-CoV-2 infection in the absence of specific antibodies, Molecular Therapy (2024), https://doi.org/10.1016/j.ymthe.2024.04.019

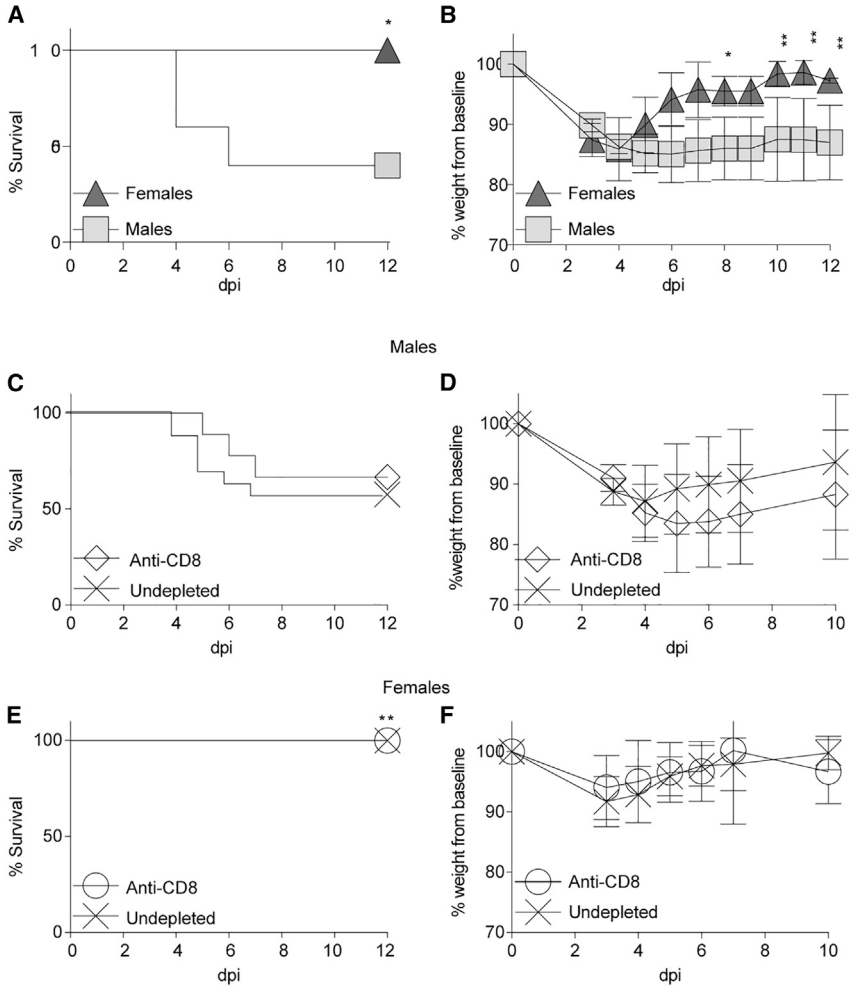

Figure 1. CD8+ T cells are not required for intrinsic resistance or susceptibility to COVID-19-like disease in mice

(A–C) Mid-aged B6 male and female mice were infected intranasally with 50,000 plaque-forming units of SARS-CoV-2 MA30 and were observed for survival (A) and weight loss (B).n = 5. Data representative of two independent experiments. (C–F) Mid-aged B6 males (C and D) and females (E and F) were depleted or not of CD8+ T cells, challenged with 50,000 pfu of MA30, and observed for survival. (C and E) and weight loss (D and F). For B6 males, n = 16 undepleted, n = 9 depleted. No significant difference was observed in depleted and undepleted males' survival or weight changes. Data were compiled from two independent experiments. For B6 females, n = 9 undepleted, n = 8 depleted per group. Data representative of two independent experiments. Statistical analysis between groups was performed using the Mann-Whitney test. *$p < 0.05$, **$p < 0.01$, ***$p < 0.001$.

suggested that a shorter prime-boost interval and i.m. immunization could be used for the SARS-CoV-2 mRNA-LNP vaccines.

The two most immunodominant CD8+ T cell epitopes described for the Spike of SARS-CoV-1 in B6 mice are the H-2 K^b restricted VNFNFNGL and YNYLYRLF.[45–47] These two epitopes are highly conserved in beta-coronaviruses, including SARS-CoV-2.[31,40,42,43,45,46,55] In preliminary experiments, we immunized mice with 1 μg S-2P mRNA LNP (the weight indicates the amount of mRNA) i.d. At 7 days post-immunization, we used H-2 K^b tetramers loaded with the corresponding peptides to measure the K^b-VNFNFNGL-, K^b-YNYLYRLF-, and control K^b-SIINFEKL (from chicken ovalbumin)-specific CD8+ T cell responses in peripheral blood. We found that B6 mice mounted CD8+ T cell responses specific for K^b-VNFNFNGL and K^b-YNYLYRLF. However, those against K^b-VNFNFNGL were significantly stronger (Figure S3). Thus, in subsequent experiments, we focused on K^b-VNFNFNGL-specific CD8+ T cell responses.

We prime-boosted mice with 10 μg S-2P mRNA-LNP i.d. or i.m. at 7-, 14-, or 28-day intervals. At 7–28 dpb, all i.m. and i.d. regimes induced mostly similar CD8+ T cell responses to VNFNFNGL as measured with K^b-VNFNFNGL tetramers (Figures 2A–2C). The only difference was at 28 dpb following a 14-day prime-boost interval when i.d.-immunized mice had significantly higher frequencies of VNFNFNGL-specific CD8+ T cells than i.m.-immunized mice (Figure 2B). There were no differences in the frequencies of central memory (cm) $CD62L^+$ $CD127^+$ and effector memory (em) $CD62^-$ $CD127^+$ CD8+ T cells[6,7,56] between the different groups (Figure S4).

Notably, at 28 dpb, the endpoint titers of anti-Spike RBD Abs measured by enzyme-linked immunosorbent assay (ELISA) did not differ significantly between groups (Figure 2D). Thus, CD8+ T cell and Ab responses to 10 μg S-2P mRNA-LNP induced by i.m. or i.d. immunization with prime-boost intervals of 7, 14, or 28 days were remarkably similar. Based on these results, we used the i.m. route with a 7-day boost interval for subsequent experiments.

A 10-fold reduction in the dose of mRNA-LNP does not significantly decrease the CD8+ T cell and antibody responses

In our published experiments and those above, we used a dose of 10 μg of mRNA-LNP.[34] However, 1 μg of the Moderna mRNA-1273 SARS-CoV-2 vaccine induced pseudovirus-nAb titers in mice that were similar in magnitude to those induced in humans with the approved human dose of 100 μg.[57,58] Therefore, we compared immune responses induced by 10 μg of S-2P mRNA-LNPs with those elicited with the more relevant 1 μg dose in mice. At 7–28 dpb, 1 and 10 μg of S-2P induced similar frequencies of K^b-$VNFNFNGL^+$ CD8+ T cells in the peripheral blood (Figure 3A). Moreover, the 1 and 10 μg doses induced similar frequencies of $CD62L^+$ $CD127^+$ cmCD8+ T cells and $CD62L^-$ $CD127^+$ emCD8+ T cells

Please cite this article in press as: Montoya et al., mRNA-LNP vaccine-induced CD8+ T cells protect mice from lethal SARS-CoV-2 infection in the absence of specific antibodies, Molecular Therapy (2024), https://doi.org/10.1016/j.ymthe.2024.04.019

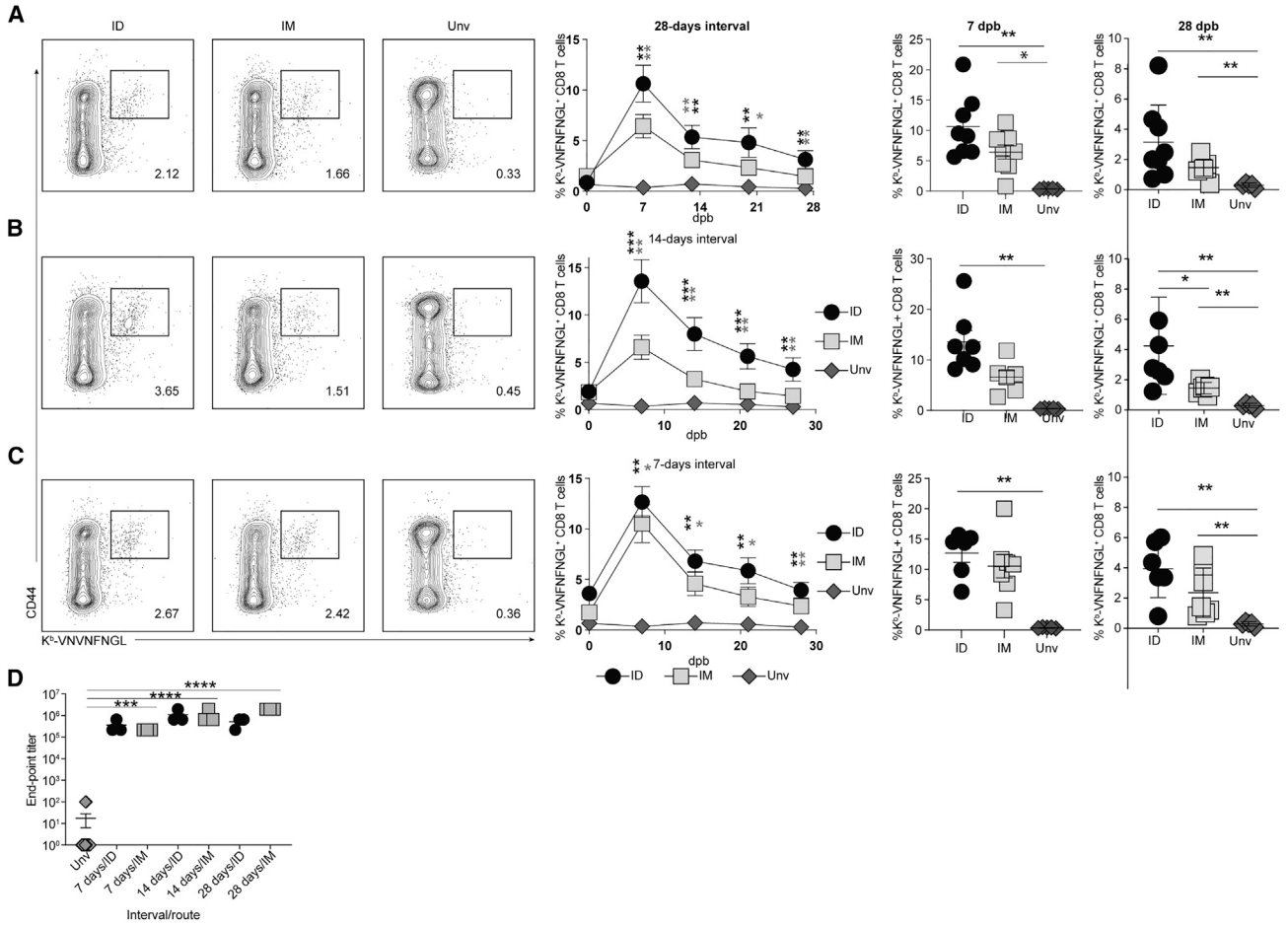

Figure 2. The prime-boost interval does not affect the CD8+ T cell or antibody responses to 10 μg S-2P mRNA-LNP in mice.

B6 mice were primed and boosted i.m. or i.d. with 10 μg S-2P mRNA-LNP. Their CD8+ T-cell and Ab responses were determined as indicated.

(A–C) K^b-VNFNFNGL-specific CD8+ T cell response with prime-boost of 28- (A), 14- (B), or 7-day (C) intervals. Representative flow cytometry plots showing CD44 and K^b-VNFNFNGL tetramer staining of gated live singlets that were CD45+ TCR-β+ CD8+ T cells at 7 and 28 dpb as indicated are shown. The overall kinetics of the K^b-VNFNFNGL-specific CD8+ T cell responses are shown on the line graphs, and the responses at 7 and 28 dpb are expanded with individual mice in the dot plots.

(D) The RBD-specific antibody titers were determined by endpoint dilution ELISA. n = 6–9 mice per group. Symbols represent individual animals. Data are compiled from two independent experiments representing eight mice for vaccinated and five for unvaccinated groups. Data shown are mean + SEM. In (A)–(C), the groups were compared using one-way ANOVA with Tukey's post-tests. All statistical differences are compared with the unvaccinated groups unless otherwise stated. Black stars indicate the significance of comparisons between i.d. and unvaccinated. Gray stars indicate the significance of comparisons between the i.m. and unvaccinated groups. *$p < 0.05$, **$p < 0.01$, ***$p < 0.001$, ****$p < 0.0001$.

(Figures 3B–3D). In addition, at 28 dpb, the RBD Ab endpoint ELISA titers in the 1 and 10 μg groups were similar (Figure 3E). These results suggest that 1 μg mRNA-LNP is sufficient for maximal CD8+ T cell and Ab responses to S-2P in B6 mice.

VNFNFNGL mini-mRNA and S-2P mRNA-LNPs induce similar frequencies of CD8+ T cells

SARS-CoV-2 antibody epitopes are more likely to mutate than CD8+ T cell epitopes. For example, sera from people prime-boosted with BNT162b2 mRNA-LNP have 34-fold less neutralizing efficiency against the SARS-CoV-2 variant B.1.1.529 (Omicron) than against the B.1 strain 1–3 months after two immunizations.[59] This is partly due to the 15 novel mutations in the Omicron RBD compared with the Wuhan-1 RBD.[60] However, CD8+ T cell epitopes are largely conserved in variants of concern.[61–63] Whether CD8+ T cells induced by SARS-CoV-2 mRNA-LNP vaccines can protect from COVID-19 is unknown. Therefore, we sought to test the efficacy of an mRNA-LNP vaccine that only induces CD8+ T cell responses.

We produced mRNA-LNPs loaded with mini-RNA encoding only VNFNFNGL (preceded by a methionine for translation initiation). We found that prime-boost doses of 1 and 10 μg induced similar frequencies of total K^b-VNFNFNGL+ CD8+ T cells at 7–28 dpb

Please cite this article in press as: Montoya et al., mRNA-LNP vaccine-induced CD8+ T cells protect mice from lethal SARS-CoV-2 infection in the absence of specific antibodies, Molecular Therapy (2024), https://doi.org/10.1016/j.ymthe.2024.04.019

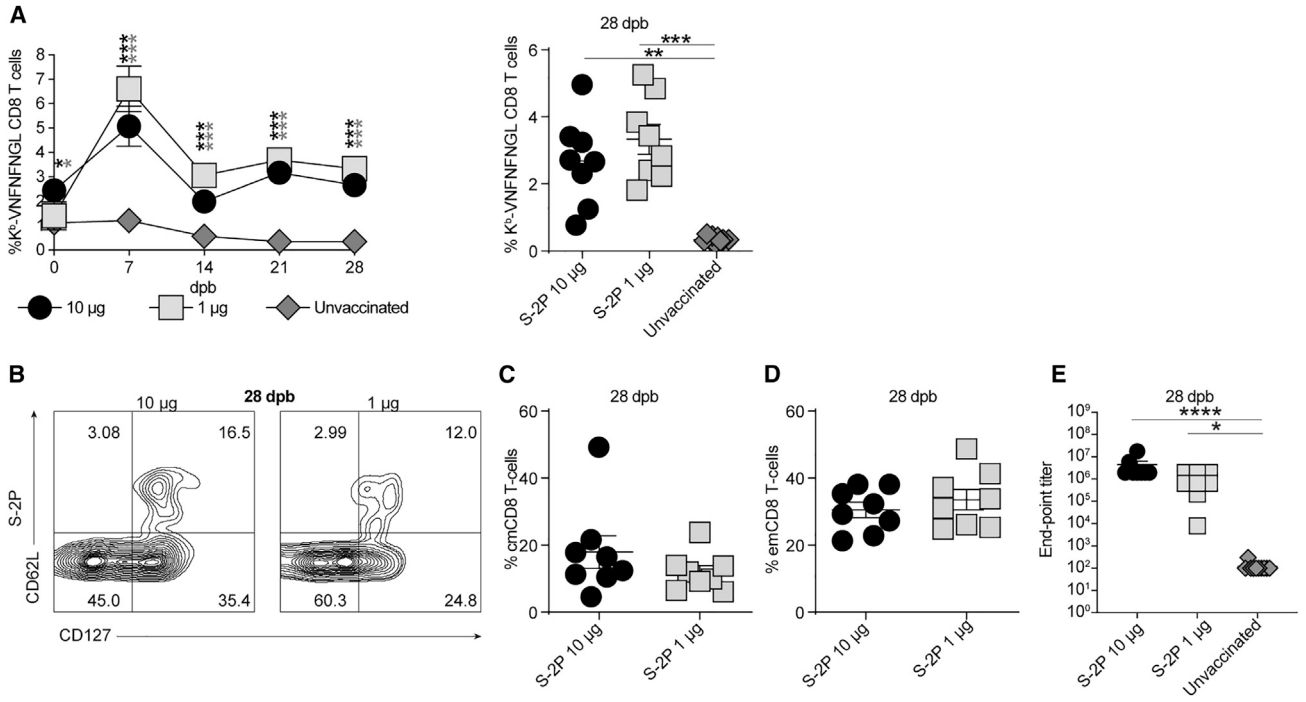

Figure 3. A 10-fold reduction in the dose of mRNA-LNP does not decrease CD8+ T cell and antibody responses in mice

Mice were primed and boosted i.m. 7 days apart with 10 or 1 µg S-2P mRNA-LNP. Their CD8+T-cell responses were analyzed as indicated.

(A) Overall kinetics of the K^b-VNFNFNGL-specific $CD8^+$ T cell responses are shown on the line graphs, and the responses at 28 dpb are expanded with individual mice in the dot plots.

(B) Representative flow cytometry plots showing CD62 and CD127 staining of gated live singlets that were $CD45^+$ TCR-β^+ $CD8^+$ $CD44^+$ K^b-VNFNFNGL$^+$ $CD8^+$ T cells in the peripheral blood of mice at 28 dpb with the indicated doses of S-2P mRNA-LNP.

(C) Frequency of $CD62L^+$ $CD127^+$ cmCD8$^+$ T cells in the indicated groups at 28 dpb.

(D) Frequency of $CD62L^-$ $CD127^+$emCD8$^+$ T cells in the indicated groups at 28 dpb.

(E) RBD-specific antibody endpoint titers as determined by ELISA at 28 dpb. n = 8 mice per group. Data representative of two independent experiments. Data shown are mean + SEM. In (A) and (C)–(E), the groups were compared using one-way ANOVA with Tukey's post-tests. There were no significant differences between vaccinated groups. *$p < 0.05$, **$p < 0.01$, ***$p < 0.001$, ***$p < 0.0001$.

(Figure 4A) and similar cmCD8$^+$ and emCD8$^+$ T cell proportions (Figures 4B–4D). These results demonstrate that, at 28 dpb, 1 and 10 µg of VNFNFNGL mRNA-LNP induce similar $CD8^+$ T cell responses. As expected, VNFNFNGL mRNA-LNP immunization did not induce Spike-specific antibodies at either dose as measured by flow cytometry using HEK293T cells transiently transfected with plasmid Spike Display B.1.1.7[64] (Figure 4E). In addition, sera from mice immunized with S-2P but not with VNFNFNGL mRNA-LNP neutralized Wuhan-1 SARS-CoV-2 (Figure 4F).

CD8+ T cells induced by SARS-CoV-2 mRNA-LNP vaccination protect B6 mice from MA30 lethality

Next, we determined whether $CD8^+$ T cells induced by mRNA-LNP immunization can protect male B6 mice from MA30 infection. We prime-boosted 60–100-day-old male B6 mice with 1 µg S-2P or VNFNFNGL mRNA-LNPs i.m. At 60–80 dpb (140–180 days old), groups of vaccinated mice were depleted or not of $CD8^+$ T cells with 100 µg anti-CD8α mAb 2.43. We then challenged all the groups with MA30 intranasally. All the unvaccinated mice experienced ~20% weight loss, and ~50% succumbed to the infection (Figures 5A–5C). Whether depleted of $CD8^+$ T cells or not, all the mice vaccinated with S-2P mRNA-LNP maintained their weight (Figure 5A) and survived the infection (Figure 5C), indicating that CD8 T cells are unnecessary, and that the antibodies induced by S-2P mRNA-LNP are sufficient to protect mice from lethal infection with the MA30 virus. On the other hand, whether $CD8^+$ T cell depleted or not, VNFNFNGL mRNA-LNP-vaccinated mice lost as much weight as unvaccinated mice (Figure 5B). However, the undepleted, but not the $CD8^+$ T cell-depleted, VNFNFNGL mRNA-LNP-vaccinated mice were significantly protected from MA30-induced lethality (Figure 5C). In addition, at 5 days post-infection (dpi), the viral titers in the lungs of $CD8^+$ T cell-depleted and -undepleted mice vaccinated with S-2P mRNA-LNP were similar and significantly lower than in unvaccinated mice (Figure 5D). These data demonstrate that the $CD8^+$ T cells induced by VNFNFNGL mRNA-LNP can protect from MA30-induced lethality when S-2P-specific antibodies are absent.

Please cite this article in press as: Montoya et al., mRNA-LNP vaccine-induced CD8+ T cells protect mice from lethal SARS-CoV-2 infection in the absence of specific antibodies, Molecular Therapy (2024), https://doi.org/10.1016/j.ymthe.2024.04.019

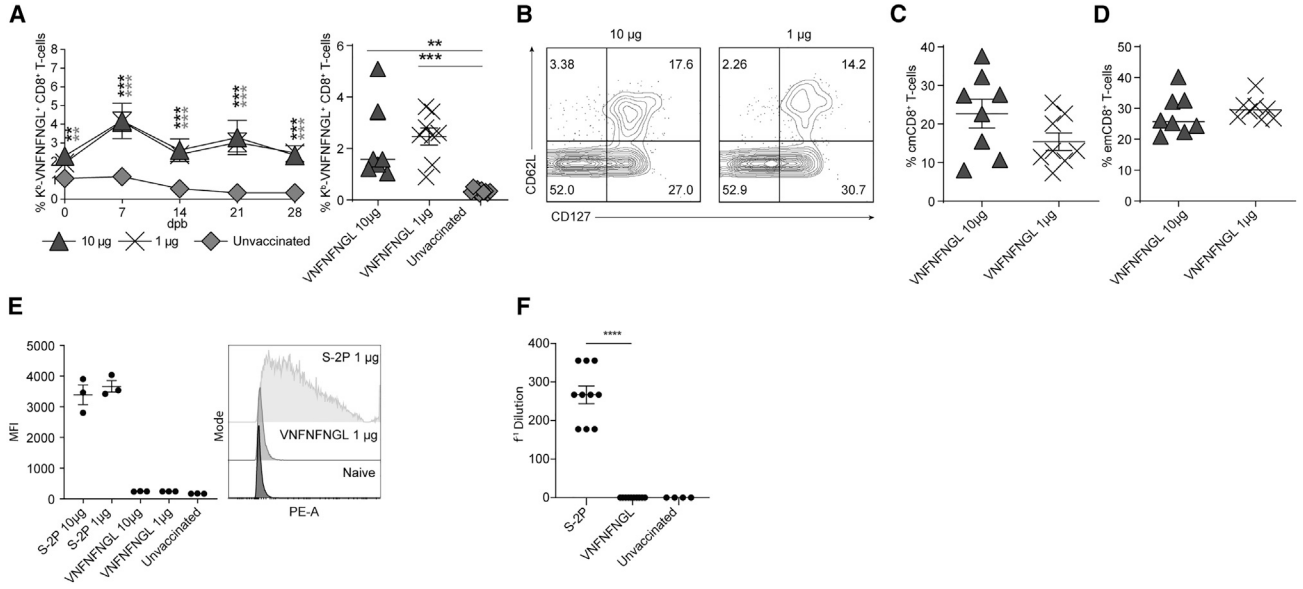

Figure 4. VNFNFNGL and S-2P mRNA-LNPs induce similar frequencies of CD8$^+$ T cells

Mice were primed and boosted i.m. 7 days apart with 10 or 1 µg VNFNFNGL mRNA-LNP. Their CD8$^+$ T-cell and Ab responses were determined as indicated.

(A) Overall kinetics of the K^b-VNFNFNGL-specific CD8$^+$ T cell responses are shown on the line graphs, and the responses at 28 dpb are expanded with individual mice in the dot plots.

(B) Representative flow cytometry plots showing CD62 and CD127 staining of gated live singlets that were CD45$^+$ TCR-β$^+$ CD8$^+$ CD44$^+$ K^b-VNFNFNGL$^+$ CD8$^+$ T cells in the peripheral blood of mice at 28 dpb with the indicated doses of VNFNFNGL mRNA-LNP. K^b-VNFNFNGL-specific CD8$^+$ T cell in peripheral blood at 28 dpb.

(C) Frequency of CD62L$^+$ CD127$^+$ cmCD8$^+$ T cells in the indicated groups at 28 dpb.

(D) Frequency of CD62L$^-$ CD127$^+$emCD8$^+$ T cells in the indicated groups at 28 dpb. n = 8 mice per group. Data representative of two independent experiments. Data shown are mean + SEM.

(E) Spike protein binding assay to determine the presence of antibodies in the serum of mice vaccinated as indicated.

(F) SARS-CoV2 Wuhan-1 neutralization by serum from the peripheral blood of mice 28 dpb. n = 10 for vaccinated groups. Data are shown as the inverse dilution at which viral infection of Vero E6 cells was observed. In (A) and (C)–(E), the groups were compared using one-way ANOVA with Tukey's post-tests. There were no significant differences between vaccinated groups for (A) and (C). *$p < 0.05$, **$p < 0.01$, ***$p < 0.001$, ****$p < 0.0001$.

CD8$^+$ T cells induced by SARS-CoV-2 mRNA-LNP vaccination protect K18-hACE2 transgenic mice from Wuhan-1-induced lethality

hACE2 protein is the functional receptor used by SARS-CoV-2 to enter human cells.[23,65] K18-hACE2 transgenic mice express the hACE2 receptor driven by the human K18 promoter and are susceptible to Wuhan-1 virus infection regardless of sex.[48,49] To test the effectiveness of a CD8$^+$ T cell vaccine against a human-relevant SARS-CoV-2 strain, we immunized K18-hACE2 female mice i.m. with 1 µg S-2P, VNFNFNGL, or control firefly luciferase (Luc)-encoding mRNA-LNP. S-2P and VNFNFNGL mRNA-LNPs induced similar CD8$^+$ T cell responses and memory differentiation in peripheral blood (Figures 6A–6D) and the lungs, inguinal (draining) lymph nodes, and spleens at 28 dpb (Figure 6E). Following intranasal infection with 1×10^4 pfu of Wuhan-1, all the mice immunized with control Luc mRNA-LNP began to lose weight at 4 dpi to reach more than 20% weight loss at 7 dpi. The experiment was then terminated due to animal welfare protocol requirements. Mice immunized with S-2P mRNA-LNP maintained their weight at all times. The mice immunized with VNFNFNGL mRNA-LNPs experienced intermediate weight loss only at 6 and 7 dpi, never reaching 20% weight loss (Figure 6F). The lungs were collected from various groups of mice and analyzed for virus titers at 2, 4, and 7 dpi. The mice immunized with Luc mRNA-LNP had high virus titers at all time points, with the highest values at 4 dpi and the lowest at 7 dpi (Figure 6G). The mice immunized with S-2P mRNA-LNP had undetectable virus titers at all time points (Figure 6G), indicating a high level of protection. The mice immunized with VNFNFNGL mRNA-LNP had virus titers similar to those in mice immunized with Luc mRNA-LNP at 2 and 4 dpi. Importantly, lung virus replication was almost undetectable at 7 dpi (Figure 6G), suggesting that CD8$^+$ T cells contribute to virus control in the late but not early phases of the infection. Together, the data with Wuhan-1 virus challenge in K18-hACE2 transgenic mice confirm the findings with the MA30 virus in B6 mice that CD8$^+$ T cells induced by mRNA-LNP vaccines reduce SARS-CoV-2 disease, although less robustly than antibodies.

DISCUSSION

The finding that the MA30 virus causes disease and lethality in male but not female mice is consistent with the higher susceptibility of men

Please cite this article in press as: Montoya et al., mRNA-LNP vaccine-induced CD8+ T cells protect mice from lethal SARS-CoV-2 infection in the absence of specific antibodies, Molecular Therapy (2024), https://doi.org/10.1016/j.ymthe.2024.04.019

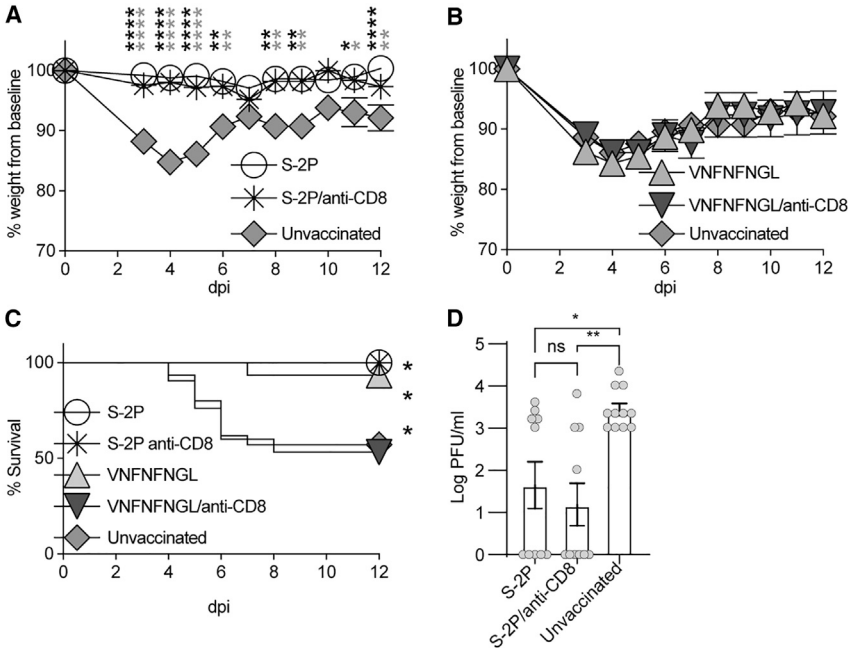

Figure 5. CD8+ T cells induced by SARS-CoV-2 mRNA-LNP vaccines protect B6 mice from MA30 virus-induced lethality

(A–C) (A) Sixty- to 100-day-old B6 mice were primed and boosted i.m. 7 days apart with 1 μg of the indicated mRNA-LNPs or left unvaccinated. At 87 dpb (147–187 days old), the indicated groups were depleted of CD8+ T cells (ΔCD8+). All groups were challenged 3 days later with 50,000 pfu SARS-CoV-2 MA30 and observed for survival. (A and B) Weight of the indicated groups at different dpi. (D) The lung viral titers of S-2P vaccinated mice depleted or undepleted of CD8 T cells and challenged with MA30 5 dpi. Groups were compared using one-way ANOVA and post hoc Mann-Whitney test. *$p < 0.05$, **$p < 0.01$, ***$p < 0.001$. In (C), S-2P and S-2P ΔCD8+ were compared with unvaccinated, VNFNFNGL was compared with VNFNFNGL ΔCD8+ and unvaccinated. In (A), the black stars indicate comparisons between S-2P mRNA-LNP-immunized and unvaccinated mice, and the gray stars between S-2P mRNA-LNP-vaccinated-ΔCD8+ and unvaccinated groups. Data representative of two experiments combined n = 13 for S-2P, *N* = 14 for S-2P ΔCD8+, n = 15 for VNFNFNGL and VNFNFNGL ΔCD8+, n = 14 for unvaccinated. For (D), n = 10 for depleted and undepleted groups, n = 11 for unvaccinated controls. Statistical analysis between groups was performed using Kruskal-Wallis and a post hoc Mann-Whitney test. *$p < 0.05$, **$p < 0.01$, ***$p < 0.001$.

to serious or fatal COVID-19.[66] This sex-dependent difference to SARS-CoV-2-induced disease has also been observed in the Syrian hamster model.[67] Similarly, female mice infected with SARS-CoV-1 have increased resilience to disease compared with age-matched male mice due to the presence of the estrogen receptor.[68] Differences in androgen production and type I interferon auto-antibodies were associated with severe COVID-19 in men.[69,70] While out of this project's scope, future studies could be conducted with the MA30 mouse model to understand the mechanisms dictating sex-related resistance to SARS-CoV-2.

The finding that CD8+ T cells do not contribute to the intrinsic resistance of female or susceptibility of male mice to SARS-CoV-2 disease or lethality is different than what is observed for influenza virus infections,[6,9] which, similar to SARS-CoV-2, causes acute respiratory distress syndrome.

In previous work, we demonstrated that mRNA-LNPs could be a powerful platform for inducing strong CD8+ T cell responses that protect against poxvirus infections.[34] Recently, mRNA-LNP vaccines against mpox virus (MPXV) have been shown to induce T cell responses to MPXV antigens, highlighting the potential for this platform to induce protective CD8+ T cell responses.[71] Here, we built upon our work to optimize a rapid immunization regime, determine the importance of the dose, and investigate whether CD8+ T cell-specific vaccines can protect susceptible mice from SARS-CoV-2 and whether the CD8+ T cells induced by the S-2P mRNA vaccine contribute to or are necessary for their capacity to induce protection against SARS-CoV-2.

It has been shown previously that VNFNFNGL-specific CD8+ T cells induced by intravenous immunization with peptide-pulsed dendritic cells followed by an intranasal booster with recombinant vaccinia virus protected K18-hACE2 mice from SARS-CoV-1.[72] It has only recently been established that T cells in general, and CD8+ T cells in particular, can protect from SARS-CoV-2 infection. For example, it has been shown that a single-epitope synthetic peptide VNFNFNGL vaccine required three doses to protect K18-hACE2 mice from SARS-CoV-2/human/NLD/Leiden-0008/2020.[42] More recently, another group showed protection of K18-hACE mice from challenge with the D614 and several Omicron variants of SARS-CoV-2 with dendritic cells transduced *ex vivo* or direct intravenous injection of a lentiviral vector expressing single CD8+ T cell epitopes from the D614 SARS-CoV-2 Spike, nucleocapsid, or ORF1.[40] In addition, we have recently shown that K18-hACE2 and BALB/c mice were respectively protected from Wuhan-1 and MA30 viruses after immunization with an mRNA vaccine containing hundreds of predicted T cell epitopes derived from all SARS-CoV-2 genes except Spike.[73] Also, Tai et al. recently demonstrated that humanized HLA transgenic mice vaccinated with mRNA-LNP encoding three SARS-CoV-2 proteome regions enriched in human HLA-1 epitopes strengthen vaccine effectiveness as indicated by lower lung viral loads and lung pathology 4 days after SARS-CoV-2 intranasal challenge.[74] Thus, clarifying whether Spike epitope-specific CD8+ T cells induced by mRNA-LNP vaccination could protect from SARS-CoV-2 challenge was important.

In initial experiments, we investigated whether the interval between prime and boost or vaccination route affects the CD8+ T cell and

Please cite this article in press as: Montoya et al., mRNA-LNP vaccine-induced CD8+ T cells protect mice from lethal SARS-CoV-2 infection in the absence of specific antibodies, Molecular Therapy (2024), https://doi.org/10.1016/j.ymthe.2024.04.019

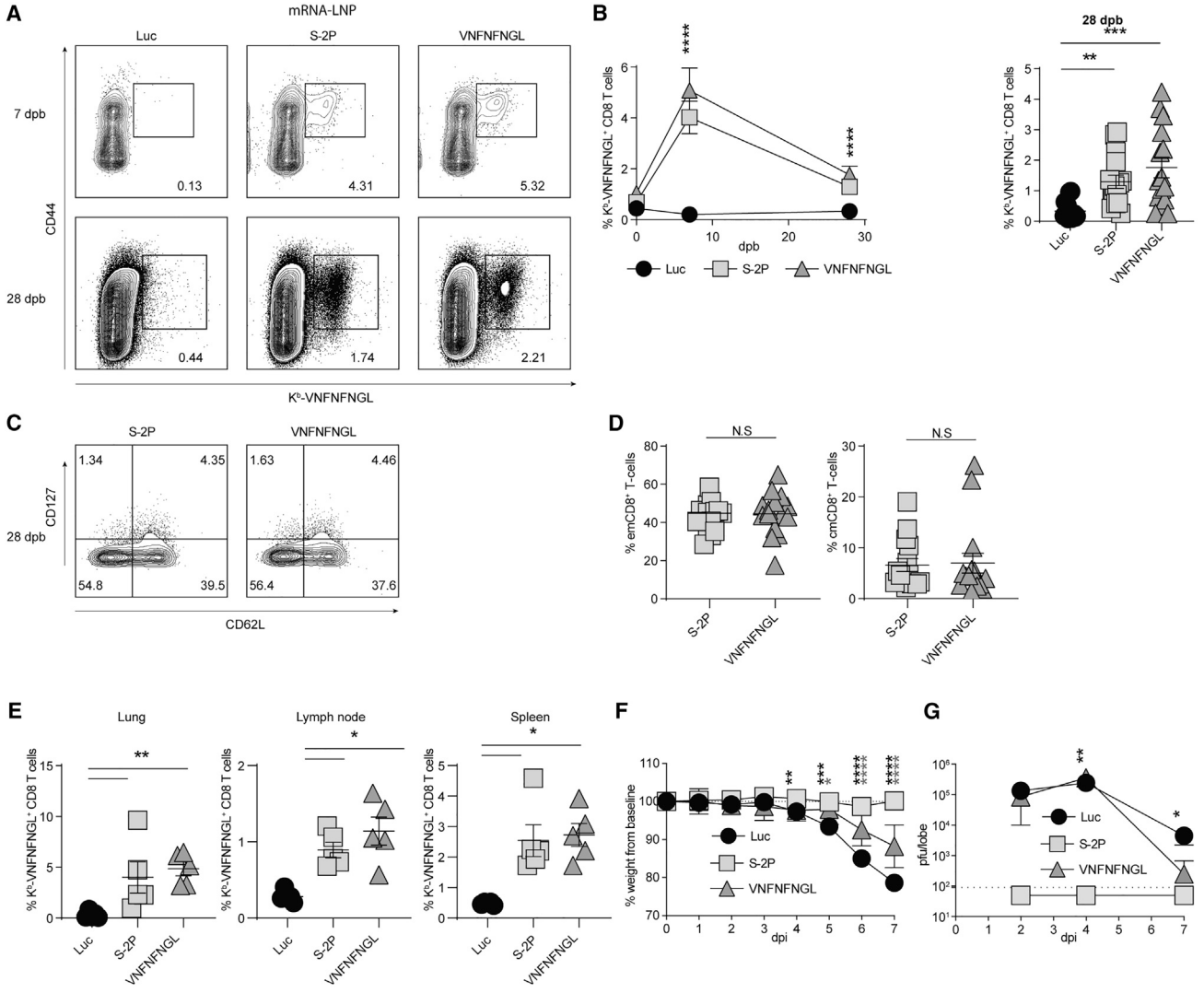

Figure 6. S-2P and VNFNFNGL mRNA-LNP vaccines protect K18 hACE2 transgenic mice from lethal Wuhan-1 infection, but only S-2P mRNA-LNP protects from weight loss

K18-hACE2 transgenic mice were primed and boosted i.m. 7 days apart with 1 μg of the indicated mRNA-LNPs. At 28 dpb, they were challenged with 10,000 pfu of the SARS CoV-2 Wuhan-1 strain.

(A) Representative flow cytometry plots showing CD44 and K^b-VNFNFNGL tetramer staining of gated live singlets that were $CD45^+$ TCR-β^+ $CD8^+$ T cells at 7 and 28 dpb.

(B) The line graph shows the kinetics of K^b-VNFNFNGL-specific $CD8^+$ T cell response in mice vaccinated as indicated, and the dot plot shows the frequencies of K^b-VNFNFNGL-specific $CD8^+$ T cell in individual mice of the different groups at 28 dpb.

(C) Representative flow cytometry plots for CD62L and CD127 staining in gated live singlets that were $CD45^+$ TCR-β^+ $CD8^+$ $CD44^+$ K^b-VNFNFNGL$^+$ at 28 dpb.

(D) Frequencies of $emCD8^+$ ($CD127^+$ $CD62^-$) (left) and $cmCD8^+$ ($CD127^+$ $CD62^+$) (right) among the K^b-VNFNFNGL$^+$ $CD8^+$ T cells in mice immunized as indicated.

(E) Lungs, inguinal lymph nodes, and spleens were harvested from five mice in the indicated mRNA-LNP vaccination groups and analyzed for K^b-VNFNFNGL-specific $CD8^+$ T cells as in (A).

(F) Mice in the indicated mRNA-LNP vaccination groups were challenged with 1×10^4 pfu SARS-CoV-2 Wuhan-1 strain and weighed on the indicated dpi.

(G) Viral lung titers from mice in the indicated mRNA-LNP vaccination groups at the indicated dpi. n = 15 per group. Data obtained from one experiment. Groups were compared using one-way ANOVA. $^*p < 0.05$, $^{**}p < 0.01$, $^{***}p < 0.001$. In (B) and (E), significant differences were only found when comparing the VNFNFNGL or S-2P with the Luc mRNA-LNP controls. In (F), the black stars indicate significant differences between S-2P and Luc, and the gray stars are between the VNFNFNGL and Luc mRNA LNP-vaccinated mice. In (G), the stars indicate significant differences between S-2P or VNFNFNGL compared with Luc mRNA-LNP immunized mice.

antibody responses to the S-2P vaccine. We found that the kinetics of the $CD8^+$ T cell response, the frequencies of VNFNFNGL-specific $CD8^+$ T cells, and the endpoint Ab titers at 28 dpb were similarly potent when the mice were primed and boosted with 10 μg S-2P mRNA-LNPs at intervals of 7, 14, or 28 days. We also found similar responses when the vaccine was given i.m. or i.d. Notably, 10 μg may

Please cite this article in press as: Montoya et al., mRNA-LNP vaccine-induced CD8+ T cells protect mice from lethal SARS-CoV-2 infection in the absence of specific antibodies, Molecular Therapy (2024), https://doi.org/10.1016/j.ymthe.2024.04.019

be saturating the CD8+ T cell responses to VNFNFNGL in mice. Lowering the vaccine dosage may result in differences for these different conditions. The original prime-boost schedule for the Moderna and Pfizer COVID-19 vaccines indicated prime and boost (so-called first and second primary doses) 3–6 weeks apart. Recent clinical data showed that a prime-boost 8–16 weeks apart resulted in 50% higher plaque reduction neutralization test (PRNT50) and PRNT90 titers against ancestral and Alpha, Beta, and Delta variants of SARS-CoV-2 but similar T cell responses when compared with the standard group, suggesting that an extended interval could be beneficial[75,76] However, full protection is not achieved with one dose, and an extended interval may be problematic when the risk of exposure is high, such as during a pandemic. Our data suggest that a short 1-week interval with the 10 μg dose is as effective as the standard in a mouse model. Because this regime results in very high (∼10% VNFNFNGL-specific CD8+ T cells), as early as 15 days post-prime, our data suggest a short interval could be considered to hasten protection in at-risk populations.

When optimizing vaccine dosage, we found that decreasing the 10 μg dose to 1 μg, which in mice induces antibody responses equivalent to those in humans,[57,58] made no significant difference in the robustness of the CD8+ T cell and antibody responses. In addition, the cmCD8+ and emCD8+ T cell pools induced by the higher and lower doses were similar in mice vaccinated with S-2P mRNA-LNP. We also found that a mini-mRNA mRNA-LNP vaccine encoding just the immunodominant Spike CD8+ T cell epitope VNFNFNGL induces CD8+ T cells of similar potency to the full-length S-2P vaccine at the 1 and 10 μg doses. These data suggest that 1 μg of mRNA-LNP may be saturating and that higher vaccine doses cannot further increase the CD8+ T cell or Ab responses to S-2P.

In the vaccine protection experiments of B6 mice challenged with the MA30 virus, S-2P mRNA-LNPs equally protected CD8+ T cell-depleted and -undepleted mice from weight loss and lethality. These data indicate that CD8+ T cells are unnecessary for resistance in the presence of protective antibodies, confirming recent work showing that K18-hACE2 mice prime-boosted with 1 μg of the Pfizer-BioNTech SARS-CoV-2 mRNA-LNP vaccine and depleted of CD8+ T cells survived Wuhan-1 SARS-CoV-2 infection with no significant weight loss compared with undepleted controls.[29] Vaccination with VNFNFNGL mRNA-LNP protected from lethality but not from weight loss, and CD8+ T cell depletion abrogated this protection, confirming that the increased resistance to death was due to the CD8+ T cells. These data indicate that CD8+ T cells induced by two doses of only 1 μg mRNA-LNP 1 week apart can protect from lethal SARS-CoV-2 infection, albeit less effectively than antibodies. The vaccine protection experiments with the SARS-CoV-2 Wuhan-1 virus in K18-hACE2 mice supported these conclusions. Our data further demonstrate that, unlike S-2P mRNA-LNP, which provided full and early protection, the CD8+ T cells induced by VNFNFNGL mRNA-LNP protected from virus loads but mostly at later stages of the infection. A need for CD8+ T cell expansion and recruitment to the lung could explain the delayed control of virus loads by VNFNFNGL compared with S-2P mRNA-LNP immunization. This could also explain why VNFNFNGL mRNA-LNP-immunized mice initially lost weight but had significantly lower viral titers at 7 dpi.

Multiple reports have shown low levels of Omicron B1.1.529 neutralization in the sera of individuals vaccinated with the Pfizer BNT162b2. Regardless, the vaccinated individuals maintained some protection.[60,61,77–79] In the various SARS-CoV-2 variants, the CD8+ T cell epitopes are more conserved than the nAb epitopes.[61,77,80,81] Thus, it is possible that vaccine-induced CD8+ T cells could contribute to the residual protection induced by the Pfizer BNT162b2 vaccine against Omicron B1.1.529. Alternatively, the non-neutralizing effector functions of Abs induced by Wuhan-1 Spike-based S-2P mRNA-LNP immunization may be sufficient for protection against non-cross-neutralizing viral variants. This could be studied in mouse models by the adoptive transfer of neutralizing and non-nAbs in CD8+ T cell-depleted mice.

Together, our data show that CD8+ T cells do not participate in the pathogenesis of SARS-CoV-2 in naive mice and that CD8+ T cells induced by mRNA-LNP vaccines incompletely control virus or reduce disease but significantly protect mice from the lethality of SARS-CoV-2 infection. This differs from what was seen in rhesus macaques, where depletion of CD8+ T cells after Spike vaccination resulted in increased viral titers and disease severity after infection with SARS-CoV-2 strain B1.617.2 (Delta).[35] CD8+ T cell protection from mRNA-LNP vaccination may depend on the challenge strain of SARS-CoV-2. Notably, the macaques in the cited study were vaccinated with the adenovirus-based-vector vaccine AD26.COV.S. It would be interesting to see if the discrepancy in CD8+ T cell protection could vary with the vaccine platform.

In this report, the epitope-specific CD8+ T cell immunity induced by VNFNFNGL mRNA-LNP was less effective than the antibody and CD8+ T cell immunity induced with Wuhan-1 S-2P mRNA-LNP. Moreover, CD8+ T cells were unnecessary for protection from MA30 or Wuhan-1 viruses following S-2P mRNA-LNP vaccination. It remains possible that CD8+ T cells against highly conserved CD8+ T cell epitopes such as VNFNFNGL may become the main protection mechanism against newly emerging SARS-CoV-2 variants or other betacoronaviruses capable of evading the protective antibody response induced by an unmatched vaccine. Others have recently shown that vaccinating with a combination of non-Spike epitopes (BNT162b4) as a supplement to Spike-encoding BNT162b2 can protect both mice and Syrian hamsters from severe disease across a variety of SARS-CoV-2 strains.[74] Hence, our data support the idea that mRNA-LNP vaccines should aim to induce CD8+ T cell responses to safeguard against viral escape from the antibody responses.

Limitations of the study

All the experiments with the 1 μg dose were performed with the 1-week prime-boost regime. Whether a different prime-boost regime could improve the responses to the 1 μg dose is unlikely but possible.

Please cite this article in press as: Montoya et al., mRNA-LNP vaccine-induced CD8+ T cells protect mice from lethal SARS-CoV-2 infection in the absence of specific antibodies, Molecular Therapy (2024), https://doi.org/10.1016/j.ymthe.2024.04.019

It is also possible that additional boosters with the VNFNFNGL mRNA-LNP may further increase protection to levels similar to those observed with S-2P mRNA-LNP. In addition, our experiments targeted only one immunodominant $CD8^+$ T cell epitope in SARS-CoV-2. Further studies should test whether mRNA-LNP vaccines containing other conserved $CD8^+$ T cell epitopes could be fully protective. Our experiments used mouse models and do not necessarily indicate the same will occur in humans.

MATERIALS AND METHODS

mRNA-LNP production

The codon-optimized sequences for S-2P and VNFNFNGL (preceded by methionine for translation initiation) were synthesized by GenScript and cloned into an mRNA production plasmid as described previously.[32,82,83] Plasmids were linearized, and mRNAs were generated using MEGAscript T7 RNA polymerase (Ambion). mRNAs were transcribed to contain poly(A) tails of 101 nucleotides in length. Uridine 5'-triphosphates were substituted for N1-methyl pseudouridine 5'-triphosphates (TriLink), and cap1 structure was generated using CleanCap (TriLink). mRNA was purified by cellulose purification as described previously[21] and analyzed by agarose gel electrophoresis. Purified mRNAs were encapsulated in LNP using a self-assembly process by rapidly mixing an aqueous solution of mRNA at pH 4.0 with a solution of lipids dissolved in ethanol; LNP were similar in composition to those described previously,[84,85] which contain an ionizable lipid/phosphatidylcholine/cholesterol/PEG-lipid.[84] The ionizable lipid is proprietary to Acuitas Therapeutics and is described in US patent US10221127. The LNPs had a diameter of ~80 nm as measured by dynamic light scattering using a Zetasizer Nano ZS (Malvern Instruments, Malvern, UK) instrument. Immunizations with the above vaccines were done as described in the text.

Mice

All experiments were approved by Thomas Jefferson University and the University of North Carolina Institutional Animal Care and Use Committees (IACUC). Wild-type C57BL/6N (B6) mice were purchased from Charles River and bred in-house. *K18-ACE2*-overexpressing mice were purchased from Jackson Laboratory and maintained at the University of North Carolina (UNC) at Chapel Hill. For all experiments, mice were sex and age matched.

Immunizations

Mice were immunized with 10 or 1 μg doses of appropriate mRNA-LNP vaccines diluted in phosphate-buffered saline (PBS) to a total volume of 20 μL. Mice were primed in the hind leg i.m. or i.d. and boosted i.m. or i.d. with the same dose of vaccine 1, 2, or 4 weeks apart.

Viruses and infection

SARS-CoV-2 MA30 was generously provided by Dr. Stanley Perlman (University of Iowa). The virus was propagated in Vero-hACE2-TMPRSS2 cells (BEI NR-54970). Confluent monolayers growing in 175 cm^2 tissue flasks were infected at a 0.05 multiplicity of infection in minimal essential medium supplemented with 2% fetal bovine serum (FBS) and penicillin-streptavidin (Gibco) and kept at 33°C. Cultures were monitored daily until the full CPE was observed. Culture medium was cleared from cell debris by centrifugation for 10 min at 3,000 × *g* for 10 min at 4°C. Viral titers were quantified with plaque assays. Mice were anesthetized with isoflurane and infected intranasally with the indicated amount of virus in a total volume of 50 μL PBS. Animal weight and health were monitored daily. All experiments involving MA30 were performed in a biosafety level 3 (BSL3) laboratory at Thomas Jefferson University. The Thomas Jefferson University Animal Care and Use Committee approved all animal studies. Infection of K18-hACE2 mice with SARS-CoV-2 Wuhan-1 strain was performed at the UNC at Chapel Hill. All experiments handling live viruses at UNC-Chapel Hill were performed in an animal BSL-3 laboratory. Laboratory workers performing BSL-3 experiments wore powered air-purifying respirators, Tyvek coverall suits, double booties covering footwear, and double gloves. All recombinant coronavirus work was approved by the UNC Institutional Biosafety Committee. All animal work was approved by the UNC IACUC. All BSL-3 work was performed in a facility conforming to requirements recommended in the Microbiological and Biomedical Laboratories by the US Department of Health and Human Services, the US Public Health Service, and the US Center for Disease Control and Prevention, and the National Institutes of Health (NIH).

CD8 T cell depletions

$CD8^+$ T cell depletion was as before.[86] In brief, mice were administered 100 μg of anti-mouse CD8α mAb clone 2.43 (BioxCell) on −5, −1, and 5 dpi, and monitored for weight loss and survival. $CD8^+$ T cell depletion was confirmed by flow cytometry in preliminary experiments.

Virus titers

For the experiments in Figure 5, the virus was determined as tissue culture infectious dose, and the data were converted to pfu. Lungs were harvested 5 dpi into 2.0 mL tubes prefilled with 0.1 mm triple-pure high-impact zirconium beads (Benchmark Scientific) containing viral transport media (RPMI, 2% FBS, 100 μg/mL gentamicin, and 0.5 μg/mL amphotericin B). Vero E6 at 1.5^5 cells/mL were seeded into black-walled, clear-bottomed 96-well plates using normal growth medium and incubated overnight at 37°C, 5.0% CO_2. The next day, 30 μL of 10-fold serial sample dilutions was added to the cells, which were then incubated for 48 h at 37°C, 5.0% CO_2. The medium was aspirated, 50 μL/well of 4% formaldehyde was added, and the plates were incubated for 10 min at room temperature. The formaldehyde was removed, and the plates were washed three times with PBST, blocked for 1 h with blocking buffer (2% BSA, 0.02% sodium azide in 1× PBST), washed three times with PBST, and 30 μL of SARS-Nucleocapsid rabbit polyclonal Ab (Cell Signaling 26369) 1:4,000 in blocking buffer was added. After overnight incubation at 4°C, the cells were washed three times with PBST, and 30 μL goat anti-rabbit IgG (H + L) 1/1,000 Alexa Fluor 488 (Invitrogen Thermo Scientific A11034) and 1/1,000 Nuclear Stain Hoechst 33342 (Cell Signaling, no. 4082) in blocking buffer, were added. The plates were washed with PBST thrice, and fluorescence was determined with a fluorescent

microscope. Wells were scored as positive and negative according to green fluorescence. Positive control using stock virus was used to determine positive fluorescence, and a negative control was used to determine background fluorescence.

For the experiments in Figure 6, virus titers were determined by plaque assays. Confluent monolayers of Vero-hACE2-TMPRSS2 cells (BEI NR-54970), cells grown in 6-well plates were incubated with serial dilutions of virus samples (250 μL/well) at 37°C for 1 h. Next, the cells were overlaid with 1% agarose (Invitrogen) prepared with MEM supplemented with 2% FBS and 1% penicillin-streptomycin-glutamine (100×, Gibco Invitrogen). After 3 days, the cells were fixed with 4% formaldehyde for 2 h, the overlay was discarded, and samples were stained with crystal violet dye or neutral red.

SARS-CoV-2 neutralization assays

96-well plates were seeded with Vero E6 cells (100 μL per well) at a density of 25,000 cells/well 1 day before assay. Serum from mice vaccinated at the indicated time points was heat inactivated at 56°C for 30 min to inactivate complement and diluted 1:10 and then serially 1:2 in Optimem at a total volume of 30 μL. Wuhan-1 (100 pfu) diluted in 30 μL Optimem was added to serum and incubated for 1 h. The sera/virus complex was added in duplicate to the Vero cells and incubated for 48 h. The cells were then fixed with 4% formaldehyde/PBS for 15 min and washed 3× with PBST. Cells were blocked (2% BSA/PBST) for 60 min and incubated in primary antibody (anti-dsRNA J2) overnight at 4°C. Cells were washed 2× with PBS and incubated in secondary (goat anti-mouse Alexa 488 [Thermo Fisher, cat. no. A32723] and Hoescht 33342 [Thermo Fisher, cat. no. H3570) for 2 h at room temperature. Cells were washed 3× in PBST and imaged using ImagXpress Micro using a 10× objective. Four sites per well were captured and scored for viral infection.

Flow cytometry

Blood was collected in hematocrit capillary tubes containing heparin (Fisher Scientific). Serum for downstream analysis was collected from the blood by spinning down at 2,000 rpm for 10 min and collecting the supernatant. Spleens were processed into single-cell suspensions by gentle tissue dissociation using frosted microscope slides (Fisher Scientific). Livers were carefully manipulated through a stainless-steel wire mesh (88 T316 0.0035-inch diameter; TWC) in a 1.5 × 1.25-in polyvinyl chloride female trap adaptor (Nibco, no. 4804). Hepatocytes were removed following re-suspension in 37% Percoll (GE Healthcare Life Sciences) and centrifugation for 20 min at 930 relative centrifugal force at room temperature. Lungs were homogenized and incubated in Liberase (Roche). The resulting liver cell pellet, splenocytes, lung cell pellet, or blood were treated with ammonium chloride potassium buffer (155 mM NH_4Cl, 1 mM $KHCO_3$, 0.1 mM EDTA) for 5 min to lyse red blood cells and washed with RPMI 1640 medium. To prevent non-specific Fc receptor binding to Abs, cells were stained with anti-CD16/32 (Fc-Block; 2.4G2 ATCC). For extracellular staining of surface molecules, single-cell suspensions were incubated with Abs in FACS buffer for 30 min at 4°C. To detect VNFNFNGL-specific $CD8^+$ T cells, H-$2K^b$-VNFNFNGL tetramers were provided by the NIH tetramer Core Facility. Tetramers were incubated with samples for 1 h at 4°C before staining with Abs targeting CD4 (clone M4-5; BV785), $CD8^+$a (clone 53-6.7; BV711), CD44 (clone IM7; BV421 BioLegend, BUV395 BD Biosciences), CD45 (clone 30-F11; PerCP/Cy5.5), CD62L (clone MEL-14; fluorescein isothiocyanate), CD90.2 (clone 53-2.1; BV605, Pacific Blue), CD127 (clone SB/199; APC), KLRG-1 (clone 2F1/KLRG1; PE/Cy7), and TCR-β (clone H57-597; Pacific Blue). All Abs were purchased from BioLegend unless otherwise stated. Data were acquired with at least 60,000 events using the BD LSR Fortessa or BD LSR II cytometers (BD Biosciences) and analyzed with FlowJo software (BD Biosciences).

Antibody responses by flow cytometry

HEK293T cells were placed in Opti-MEM reduced serum medium (Gibco) and seeded in 12-well plates at 100k cells/well. Upon reaching ∼70% confluency, cells were transiently transfected with Spike Display B.1.1.7 cloned into pcDNA5 vector (Addgene, no. 172735) using 1.6 μg Lipofectamine 3000 reagent (Invitrogen) and 1 μg DNA per well. After transfection, the cells were incubated for 2 days at 37°C and then used to measure antibodies in serum. HEK293T cells (10^5) transiently transfected with B.1.1.7 were seeded into 96-well plates in 100 μL of complete medium. Serum (100 μL) diluted 1:10 in complete medium was overlaid on the cells and incubated at room temperature for 1 h. Cells were washed twice and stained with PE anti-mouse IgG1 (BioLegend) diluted in blocking buffer (1:400 total dilution) for 30 min. Cells were washed three times with PBS, resuspended in FACS buffer, and immediately analyzed on a BD FACSymphony A5 spectral flow cytometer.

Production of recombinant protein

The recombinant RBD-His6 (referred to as RBD) was generated in Expi293F mammalian cells, following the procedure described previously.[87] In brief, 72 h after transfection, the clarified cell culture medium was supplemented with 20 mM sodium phosphate (pH 8.0), 50 mM NaCl, and 20 mM imidazole. The medium was then sterile filtered and subjected to IMAC purification utilizing Ni Sepharose 6 Fast Flow resin (Cytiva, Washington, WA, cat. no. 17531802). Following a 2-h incubation at 4°C, the resin was washed five times with buffer A (50 mM sodium phosphate [pH 8.0], 300 mM NaCl, and 20 mM imidazole), and the RBD was eluted using buffer B (50 mM sodium phosphate [pH 8.0], 300 mM NaCl, and 300 mM imidazole). Subsequently, the purified RBD underwent buffer exchange into PBS (pH 7.4) and was concentrated to a final concentration of 1 mg/mL using an Amicon Ultra centrifugal filter unit (MWCO: 10 kDa; Merck Millipore, Burlington, MA, cat. no. UFC9010). The RBD samples were sterile filtered and stored in a −80°C freezer until required.

ELISAs

ELISAs were performed as described previously.[88] In brief, high-binding 96-well clear polystyrene plates (Corning, 3590) were coated (100 μL/well) with purified SARS-CoV-2 RBD protein in PBS (Corning, 21-031-CM) at a final concentration of 100 ng per well and allowed to incubate overnight at 4°C. Then, the plates were washed

(300 μL/well) four times with 0.1% Tween 20 (Sigma-Aldrich, P9416) in PBS and blocked (200 μL/well) in blocking buffer (2% w/v BSA [Sigma-Aldrich, A7030] in PBS) for 2 h at room temperature. After removal of the blocking buffer, sera were serially diluted in fresh blocking buffer, and the samples (100 μL/well) were incubated at room temperature for 2 h. Plates were then washed (300 μL/well) three times with PBS, and goat anti-mouse IgG (H+L) secondary antibody (Jackson ImmunoResearch, 115-035-003) was added at a concentration of 1:10,000 in blocking buffer and incubated (100 μL/well) at room temperature for 1 h. The plates were washed (300 μL/well) three times with PBS before adding 100 μL per well of KPL TMB Microwell Peroxidase Substrate System (Seracare, 5120-0047) for 8 min. The reaction was quenched with 50 μL 2N sulfuric acid (Sigma-Aldrich, 258105), and the absorbance was measured at 450 nm using a microplate reader (Molecular Devices, SpectraMax 190). Data were processed using Microsoft Excel 2019 and Prism 8.0 (GraphPad). Endpoint dilution titer was calculated as the highest serum dilution to give a value greater than the background (no serum, cut-off OD value +0.01 OD). All samples were run in technical duplicates.

Statistical analysis

Data were visualized and analyzed in Prism (v.9.5.0). Non-parametric tests were performed as described in each figure legend. Figures were assembled in Adobe Illustrator (v.27.0).

DATA AND CODE AVAILABILITY

This work did not produce datasets that must be deposited in public databanks.

SUPPLEMENTAL INFORMATION

Supplemental information can be found online at https://doi.org/10.1016/j.ymthe.2024.04.019.

ACKNOWLEDGMENTS

R56AI110457, R01AI175567, and R01AI169460 funded the Sigal laboratory. R01AI146101, R01AI153064, and P01AI158571 funded the Pardi laboratory. P01 AI158571 funded the Baric laboratory. R01AI169460 funded the Andino laboratory. The Lipinszki laboratory was funded by the Hungarian Academy of Sciences (Lendület Program Grant [LP2017-7/2017] and the National Laboratory for Biotechnology [2022-2.1.1-NL-2022-00008]). C.B. was a postdoctoral fellow in the Pardi Laboratory supported by the National Laboratory for Biotechnology (2022-2.1.1-NL-2022-00008), Szeged, Hungary. B.M. was partly funded by T32AI134646 (NIAID, NIH, USA) to L.J.S. We thank the NIH tetramer core facility for providing spike-specific tetramers for CD8+ T cell detection. We thank the Thomas Jefferson University Laboratory Animal Facility for animal care. We thank the Thomas Jefferson University BSL3/ABSL3 shared resource, the Center for Vaccines and Pandemic Preparedness, Megan Watson, and Holly Ramage for experimental and technical assistance.

AUTHOR CONTRIBUTIONS

B.M. designed and performed most of the experiments and wrote the paper. C.R.M.-S., L.T., and S.K. collaborated in experiments. P.L. produced the MA30 virus. C.B. and M.V. performed RBD-specific ELISA studies. H.M. produced all mRNAs. E.A. performed RBD cloning and expression. Z.L. performed RBD expression, purification, and validation and contributed to the funding. D.C. and G.S. collaborated in SARS-CoV-2 B6 mice challenge experiments. J.B. collaborated in the SARS-CoV-2 B6 mice challenge and flow cytometry experiments. M.M.H.S. manufactured LNPs. Y.K.T. supervised the manufacture of LNPs. R.S.B. supervised the experiments with K18-hACE2 mice with SARS-CoV-2 Wuhan-1 and contributed to the funding. D.R.M. co-designed and supervised the experiments with K18-hACE2 mice with SARS-CoV-2 Wuhan-1. R.A. supervised MA30 production and contributed to the funding. N.P. designed and supervised the production of mRNAs, co-designed the experiments with Wuhan-1, designed and supervised the ELISA experiments, and contributed to the funding. L.J.S. was responsible for the project's overall design, supervised most of the work, edited the paper, and contributed to the funding.

DECLARATION OF INTERESTS

L.J.S. is a member of the Scientific Advisory Board of RNA Advanced Technologies member. N.P. is named on patents describing the use of nucleoside-modified mRNA in LNPs as a vaccine platform. He has disclosed those interests fully to the University of Pennsylvania and has an approved plan for managing potential conflicts arising from licensing those patents. N.P. served on the mRNA strategic advisory board of Sanofi Pasteur in 2022 and Pfizer in 2023–2024, and is a member of the Scientific Advisory Board of AldexChem and BioNet and has consulted for Vaccine Company Inc. and Pasture Bio. R.S.B. is a member of the Scientific Advisory Board of Invivyd and VaxArt and has consulted on virus-related countermeasures with Gilead, Moderna, Takeda, BioNet, and Jenssen Bio unrelated to this project. Y.K.T. and M.M.H. Sung are employees of Acuitas Therapeutics.

REFERENCES

1. Rock, K.L., Reits, E., and Neefjes, J. (2016). Present Yourself! By MHC Class I and MHC Class II Molecules. Trends Immunol. *37*, 724–737. https://doi.org/10.1016/j.it.2016.08.010.

2. Wherry, E.J., Teichgräber, V., Becker, T.C., Masopust, D., Kaech, S.M., Antia, R., von Andrian, U.H., and Ahmed, R. (2003). Lineage relationship and protective immunity of memory CD8 T cell subsets. Nat. Immunol. *4*, 225–234. https://doi.org/10.1038/ni889.

3. Barber, D.L., Wherry, E.J., and Ahmed, R. (2003). Cutting edge: rapid *in vivo* killing by memory CD8 T cells. J. Immunol. *171*, 27–31. https://doi.org/10.4049/jimmunol.171.1.27.

4. Kaech, S.M., Wherry, E.J., and Ahmed, R. (2002). Effector and memory T-cell differentiation: implications for vaccine development. Nat. Rev. Immunol. *2*, 251–262. https://doi.org/10.1038/nri778.

5. Remakus, S., and Sigal, L.J. (2013). Memory CD8(+) T cell protection. Adv. Exp. Med. Biol. *785*, 77–86. https://doi.org/10.1007/978-1-4614-6217-0_9.

6. Flynn, K.J., Belz, G.T., Altman, J.D., Ahmed, R., Woodland, D.L., and Doherty, P.C. (1998). Virus-Specific CD81 T Cells in Primary and Secondary Influenza Pneumonia. Immunity *8*, 683–691.

7. Usherwood, E.J., Hogan, R.J., Crowther, G., Surman, S.L., Hogg, T.L., Altman, J.D., and Woodland, D.L. (1999). Functionally Heterogeneous CD8≦ T-Cell Memory Is Induced by Sendai Virus Infection of Mice. J. Virol. *73*, 7278–7286.
8. Moseman, E.A., and McGavern, D.B. (2013). The great balancing act: regulation and fate of antiviral T-cell interactions. Immunol. Rev. *255*, 110–124. https://doi.org/10.1111/imr.12093.
9. Duan, S., and Thomas, P.G. (2016). Balancing Immune Protection and Immune Pathology by CD8(+) T-Cell Responses to Influenza Infection. Front. Immunol. *7*, 25. https://doi.org/10.3389/fimmu.2016.00025.
10. Chisari, F.V., Isogawa, M., and Wieland, S.F. (2010). Pathogenesis of hepatitis B virus infection. Pathol. Biol. *58*, 258–266. https://doi.org/10.1016/j.patbio.2009.11.001.
11. Fang, M., and Sigal, L.J. (2005). Antibodies and CD8+ T Cells Are Complementary and Essential for Natural Resistance to a Highly Lethal Cytopathic Virus. J. Immunol. *175*, 6829–6836. https://doi.org/10.4049/jimmunol.175.10.6829.
12. Xu, R.-H., Fang, M., Klein-Szanto, A., and Sigal, L.J. (2007). Memory CD8+T cells are gatekeepers of the lymphnode draining the site of viral infection. PNAS *104*, 10992–10997.
13. Zhang, N., and Bevan, M.J. (2011). CD8(+) T cells: foot soldiers of the immune system. Immunity *35*, 161–168. https://doi.org/10.1016/j.immuni.2011.07.010.
14. Pollard, A.J., and Bijker, E.M. (2021). A guide to vaccinology: from basic principles to new developments. Nat. Rev. Immunol. *21*, 83–100. https://doi.org/10.1038/s41577-020-00479-7.
15. Hogan, M.J., and Pardi, N. (2022). mRNA Vaccines in the COVID-19 Pandemic and Beyond. Annu. Rev. Med. *73*, 17–39. https://doi.org/10.1146/annurev-med-042420-112725.
16. Andries, O., Mc Cafferty, S., De Smedt, S.C., Weiss, R., Sanders, N.N., and Kitada, T. (2015). N(1)-methylpseudouridine-incorporated mRNA outperforms pseudouridine-incorporated mRNA by providing enhanced protein expression and reduced immunogenicity in mammalian cell lines and mice. J. Control Release *217*, 337–344. https://doi.org/10.1016/j.jconrel.2015.08.051.
17. Karikó, K., Muramatsu, H., Ludwig, J., and Weissman, D. (2011). Generating the optimal mRNA for therapy: HPLC purification eliminates immune activation and improves translation of nucleoside-modified, protein-encoding mRNA. Nucleic Acids Res. *39*, e142. https://doi.org/10.1093/nar/gkr695.
18. Pardi, N., Tuyishime, S., Muramatsu, H., Kariko, K., Mui, B.L., Tam, Y.K., Madden, T.D., Hope, M.J., and Weissman, D. (2015). Expression kinetics of nucleoside-modified mRNA delivered in lipid nanoparticles to mice by various routes. J. Control Release *217*, 345–351. https://doi.org/10.1016/j.jconrel.2015.08.007.
19. Pardi, N., Hogan, M.J., Porter, F.W., and Weissman, D. (2018). mRNA vaccines - a new era in vaccinology. Nat. Rev. Drug Discov. *17*, 261–279. https://doi.org/10.1038/nrd.2017.243.
20. Weissman, D., Pardi, N., Muramatsu, H., and Karikó, K. (2013). HPLC Purification of In Vitro Transcribed Long RNA. In Synthetic Messenger RNA and Cell Metabolism Modulation: Methods and Protocols, P.M. Rabinovich, ed. (Humana Press), pp. 43–54. https://doi.org/10.1007/978-1-62703-260-5_3.
21. Baiersdörfer, M., Boros, G., Muramatsu, H., Mahiny, A., Vlatkovic, I., Sahin, U., and Karikó, K. (2019). A Facile Method for the Removal of dsRNA Contaminant from In Vitro-Transcribed mRNA. Mol. Ther. Nucleic Acids *15*, 26–35. https://doi.org/10.1016/j.omtn.2019.02.018.
22. Watson, O.J., Barnsley, G., Toor, J., Hogan, A.B., Winskill, P., and Ghani, A.C. (2022). Global impact of the first year of COVID-19 vaccination: a mathematical modelling study. Lancet Infect. Dis. *22*, 1293–1302. https://doi.org/10.1016/S1473-3099(22)00320-6.
23. Walls, A.C., Park, Y.J., Tortorici, M.A., Wall, A., McGuire, A.T., and Veesler, D. (2020). Structure, Function, and Antigenicity of the SARS-CoV-2 Spike Glycoprotein. Cell *181*, 281–292.e6. https://doi.org/10.1016/j.cell.2020.02.058.
24. Hoffmann, M., Kleine-Weber, H., Schroeder, S., Krüger, N., Herrler, T., Erichsen, S., Schiergens, T.S., Herrler, G., Wu, N.H., Nitsche, A., et al. (2020). SARS-CoV-2 Cell Entry Depends on ACE2 and TMPRSS2 and Is Blocked by a Clinically Proven Protease Inhibitor. Cell *181*, 271–280.e8. https://doi.org/10.1016/j.cell.2020.02.052.
25. Dai, L., and Gao, G.F. (2021). Viral targets for vaccines against COVID-19. Nat. Rev. Immunol. *21*, 73–82. https://doi.org/10.1038/s41577-020-00480-0.
26. Pallesen, J., Wang, N., Corbett, K.S., Wrapp, D., Kirchdoerfer, R.N., Turner, H.L., Cottrell, C.A., Becker, M.M., Wang, L., Shi, W., et al. (2017). Immunogenicity and structures of a rationally designed prefusion MERS-CoV spike antigen. Proc. Natl. Acad. Sci. USA *114*, E7348–E7357. https://doi.org/10.1073/pnas.1707304114.
27. Walsh, E.E., Frenck, R.W., Jr., Falsey, A.R., Kitchin, N., Absalon, J., Gurtman, A., Lockhart, S., Neuzil, K., Mulligan, M.J., Bailey, R., et al. (2020). Safety and Immunogenicity of Two RNA-Based Covid-19 Vaccine Candidates. N. Engl. J. Med. *383*, 2439–2450. https://doi.org/10.1056/NEJMoa2027906.
28. Polack, F.P., Thomas, S.J., Kitchin, N., Absalon, J., Gurtman, A., Lockhart, S., Perez, J.L., Pérez Marc, G., Moreira, E.D., Zerbini, C., et al. (2020). Safety and Efficacy of the BNT162b2 mRNA Covid-19 Vaccine. N. Engl. J. Med. *383*, 2603–2615. https://doi.org/10.1056/NEJMoa2034577.
29. Israelow, B., Mao, T., Klein, J., Song, E., Menasche, B., Omer, S.B., and Iwasaki, A. (2021). Adaptive immune determinants of viral clearance and protection in mouse models of SARS-CoV-2. Sci. Immunol. *6*, eabl4509.
30. Martinez, D.R., Schäfer, A., Leist, S.R., De la Cruz, G., West, A., Atochina-Vasserman, E.N., Lindesmith, L.C., Pardi, N., Parks, R., Barr, M., et al. (2021). Chimeric spike mRNA vaccines protect against Sarbecovirus challenge in mice. Science *373*, 991–998. https://doi.org/10.1126/science.abi4506.
31. Li, C., Lee, A., Grigoryan, L., Arunachalam, P.S., Scott, M.K.D., Trisal, M., Wimmers, F., Sanyal, M., Weidenbacher, P.A., Feng, Y., et al. (2022). Mechanisms of innate and adaptive immunity to the Pfizer-BioNTech BNT162b2 vaccine. Nat. Immunol. *23*, 543–555. https://doi.org/10.1038/s41590-022-01163-9.
32. Laczkó, D., Hogan, M.J., Toulmin, S.A., Hicks, P., Lederer, K., Gaudette, B.T., Castaño, D., Amanat, F., Muramatsu, H., Oguin, T.H., 3rd, et al. (2020). A Single Immunization with Nucleoside-Modified mRNA Vaccines Elicits Strong Cellular and Humoral Immune Responses against SARS-CoV-2 in Mice. Immunity *53*, 724–732.e7. https://doi.org/10.1016/j.immuni.2020.07.019.
33. Brasu, N., Elia, I., Russo, V., Montacchiesi, G., Stabile, S.A., De Intinis, C., Fesi, F., Gizzi, K., Macagno, M., Montone, M., et al. (2022). Memory CD8(+) T cell diversity and B cell responses correlate with protection against SARS-CoV-2 following mRNA vaccination. Nat. Immunol. *23*, 1445–1456. https://doi.org/10.1038/s41590-022-01313-z.
34. Knudson, C.J., Alves-Peixoto, P., Muramatsu, H., Stotesbury, C., Tang, L., Lin, P.J.C., Tam, Y.K., Weissman, D., Pardi, N., and Sigal, L.J. (2021). Lipid-nanoparticle-encapsulated mRNA vaccines induce protective memory CD8 T cells against a lethal viral infection. Mol. Ther. *29*, 2769–2781. https://doi.org/10.1016/j.ymthe.2021.05.011.
35. Liu, J., Yu, J., McMahan, K., Jacob-Dolan, C., He, X., Giffin, V., Wu, C., Sciacca, M., Powers, O., Nampanya, F., et al. (2022). CD8 T cells contribute to vaccine protection against SARS-CoV-2 in macaques. Sci. Immunol. *7*, eabq7647. https://doi.org/10.1126/sciimmunol.abq7647.
36. Hajnik, R.L., Plante, J.A., Liang, Y., Alameh, M.-G., Tang, J., Bonam, S.R., Zhong, C., Adam, A., Scharton, D., Rafael, G.H., et al. (2022). Dual spike and nucleocapsid mRNA vaccination confer protection against SARS-CoV-2 Omicron and Delta variants in preclinical models. Sci. Transl. Med. *14*, eabq1945. https://doi.org/10.1126/scitranslmed.abq1945.
37. Remakus, S., Rubio, D., Ma, X., Sette, A., and Sigal, L.J. (2012). Memory CD8+ T cells specific for a single immunodominant or subdominant determinant induced by peptide-dendritic cell immunization protect from an acute lethal viral disease. J. Virol. *86*, 9748–9759. https://doi.org/10.1128/JVI.00981-12.
38. Remakus, S., Ma, X., Tang, L., Xu, R.H., Knudson, C., Melo-Silva, C.R., Rubio, D., Kuo, Y.M., Andrews, A., and Sigal, L.J. (2018). Cutting Edge: Protection by Antiviral Memory CD8 T Cells Requires Rapidly Produced Antigen in Large Amounts. J. Immunol. *200*, 3347–3352. https://doi.org/10.4049/jimmunol.1701568.
39. Fang, M., Remakus, S., Roscoe, F., Ma, X., and Sigal, L.J. (2015). CD4+ T cell help is dispensable for protective CD8+ T cell memory against mousepox virus following vaccinia virus immunization. J. Virol. *89*, 776–783. https://doi.org/10.1128/JVI.02176-14.
40. Tada, T., Peng, J.Y., Dcosta, B.M., and Landau, N.R. (2023). Single-epitope T cell-based vaccine protects against SARS-CoV-2 infection in a preclinical animal model. JCI Insight *8*, e167306. https://doi.org/10.1172/jci.insight.167306.
41. Kingstad-Bakke, B., Lee, W., Chandrasekar, S.S., Gasper, D.J., Salas-Quinchucua, C., Cleven, T., Sullivan, J.A., Talaat, A., Osorio, J.E., and Suresh, M. (2022).

Vaccine-induced systemic and mucosal T cell immunity to SARS-CoV-2 viral variants. Proc. Natl. Acad. Sci. USA *119*, e2118312119. https://doi.org/10.1073/pnas.2118312119.

42. Pardieck, I.N., van der Sluis, T.C., van der Gracht, E.T.I., Veerkamp, D.M.B., Behr, F.M., van Duikeren, S., Beyrend, G., Rip, J., Nadafi, R., Beyranvand Nejad, E., et al. (2022). A third vaccination with a single T cell epitope confers protection in a murine model of SARS-CoV-2 infection. Nat. Commun. *13*, 3966. https://doi.org/10.1038/s41467-022-31721-6.

43. Poluektov, Y., George, M., Daftarian, P., and Delcommenne, M.C. (2021). Assessment of SARS-CoV-2 specific CD4(+) and CD8 (+) T cell responses using MHC class I and II tetramers. Vaccine *39*, 2110–2116. https://doi.org/10.1016/j.vaccine.2021.03.008.

44. Hassert, M., Geerling, E., Stone, E.T., Steffen, T.L., Feldman, M.S., Dickson, A.L., Class, J., Richner, J.M., Brien, J.D., and Pinto, A.K. (2020). mRNA induced expression of human angiotensin-converting enzyme 2 in mice for the study of the adaptive immune response to severe acute respiratory syndrome coronavirus 2. Plos Pathog. *16*, e1009163. https://doi.org/10.1371/journal.ppat.1009163.

45. Zhao, J., Wohlford-Lenane, C., Zhao, J., Fleming, E., Lane, T.E., McCray, P.B., Jr., and Perlman, S. (2012). Intranasal treatment with poly(I*C) protects aged mice from lethal respiratory virus infections. J. Virol. *86*, 11416–11424. https://doi.org/10.1128/JVI.01410-12.

46. Zhao, J., Zhao, J., and Perlman, S. (2010). T cell responses are required for protection from clinical disease and for virus clearance in severe acute respiratory syndrome coronavirus-infected mice. J. Virol. *84*, 9318–9325. https://doi.org/10.1128/JVI.01049-10.

47. Zhi, Y., Kobinger, G.P., Jordan, H., Suchma, K., Weiss, S.R., Shen, H., Schumer, G., Gao, G., Boyer, J.L., Crystal, R.G., and Wilson, J.M. (2005). Identification of murine CD8 T cell epitopes in codon-optimized SARS-associated coronavirus spike protein. Virology *335*, 34–45. https://doi.org/10.1016/j.virol.2005.01.050.

48. Oladunni, F.S., Park, J.G., Pino, P.A., Gonzalez, O., Akhter, A., Allué-Guardia, A., Olmo-Fontánez, A., Gautam, S., Garcia-Vilanova, A., Ye, C., et al. (2020). Lethality of SARS-CoV-2 infection in K18 human angiotensin-converting enzyme 2 transgenic mice. Nat. Commun. *11*, 6122. https://doi.org/10.1038/s41467-020-19891-7.

49. Jiang, R.D., Liu, M.Q., Chen, Y., Shan, C., Zhou, Y.W., Shen, X.R., Li, Q., Zhang, L., Zhu, Y., Si, H.R., et al. (2020). Pathogenesis of SARS-CoV-2 in Transgenic Mice Expressing Human Angiotensin-Converting Enzyme 2. Cell *182*, 50–58.e8. https://doi.org/10.1016/j.cell.2020.05.027.

50. Wong, L.Y.R., Zheng, J., Wilhelmsen, K., Li, K., Ortiz, M.E., Schnicker, N.J., Thurman, A., Pezzulo, A.A., Szachowicz, P.J., Li, P., et al. (2022). Eicosanoid signalling blockade protects middle-aged mice from severe COVID-19. Nature *605*, 146–151. https://doi.org/10.1038/s41586-022-04630-3.

51. Schmidt, M.E., and Varga, S.M. (2020). Cytokines and CD8 T cell immunity during respiratory syncytial virus infection. Cytokine *133*, 154481. https://doi.org/10.1016/j.cyto.2018.07.012.

52. Davis, M.A., Voss, K., Turnbull, J.B., Gustin, A.T., Knoll, M., Muruato, A., Hsiang, T.Y., Dinnon Iii, K.H., Leist, S.R., Nickel, K., et al. (2022). A C57BL/6 Mouse Model of SARS-CoV-2 Infection Recapitulates Age- and Sex-Based Differences in Human COVID-19 Disease and Recovery. Vaccines (Basel) *11*, 47. https://doi.org/10.3390/vaccines11010047.

53. Munro, A.P.S., Janani, L., Cornelius, V., Aley, P.K., Babbage, G., Baxter, D., Bula, M., Cathie, K., Chatterjee, K., Dodd, K., et al. (2021). Safety and immunogenicity of seven COVID-19 vaccines as a third dose (booster) following two doses of ChAdOx1 nCov-19 or BNT162b2 in the UK (COV-BOOST): a blinded, multicentre, randomised, controlled, phase 2 trial. Lancet *398*, 2258–2276. https://doi.org/10.1016/S0140-6736(21)02717-3.

54. Choi, A., Koch, M., Wu, K., Chu, L., Ma, L., Hill, A., Nunna, N., Huang, W., Oestreicher, J., Colpitts, T., et al. (2021). Safety and immunogenicity of SARS-CoV-2 variant mRNA vaccine boosters in healthy adults: an interim analysis. Nat. Med. *27*, 2025–2031. https://doi.org/10.1038/s41591-021-01527-y.

55. Erez, N., Achdout, H., Yahalom-Ronen, Y., Adutler-Lieber, S., Bar-On, L., Bar-Haim, E., Politi, B., Vitner, E.B., Tamir, H., Melamed, S., et al. (2023). Identification of T-Cell Epitopes Using a Combined In-Silico and Experimental Approach in a Mouse Model for SARS-CoV-2. Curr. Issues Mol. Biol. *45*, 7944–7955. https://doi.org/10.3390/cimb45100502.

56. Sallusto, F., Lenig, D., Förster, R., Lipp, M., and Lanzavecchia, A. (1999). Two subsets of memory T lymphocytes with distinct homing potentials and effector functions. Nature *401*, 708–712.

57. Corbett, K.S., Edwards, D.K., Leist, S.R., Abiona, O.M., Boyoglu-Barnum, S., Gillespie, R.A., Himansu, S., Schäfer, A., Ziwawo, C.T., DiPiazza, A.T., et al. (2020). SARS-CoV-2 mRNA vaccine design enabled by prototype pathogen preparedness. Nature *586*, 567–571. https://doi.org/10.1038/s41586-020-2622-0.

58. Jackson, L.A., Anderson, E.J., Rouphael, N.G., Roberts, P.C., Makhene, M., Coler, R.N., McCullough, M.P., Chappell, J.D., Denison, M.R., Stevens, L.J., et al. (2020). An mRNA Vaccine against SARS-CoV-2 - Preliminary Report. N. Engl. J. Med. *383*, 1920–1931. https://doi.org/10.1056/NEJMoa2022483.

59. Hoffmann, M., Krüger, N., Schulz, S., Cossmann, A., Rocha, C., Kempf, A., Nehlmeier, I., Graichen, L., Moldenhauer, A.S., Winkler, M.S., et al. (2022). The Omicron variant is highly resistant against antibody-mediated neutralization: Implications for control of the COVID-19 pandemic. Cell *185*, 447–456.e11. https://doi.org/10.1016/j.cell.2021.12.032.

60. Cao, Y., Wang, J., Jian, F., Xiao, T., Song, W., Yisimayi, A., Huang, W., Li, Q., Wang, P., An, R., et al. (2022). Omicron escapes the majority of existing SARS-CoV-2 neutralizing antibodies. Nature *602*, 657–663. https://doi.org/10.1038/s41586-021-04385-3.

61. Tarke, A., Coelho, C.H., Zhang, Z., Dan, J.M., Yu, E.D., Methot, N., Bloom, N.I., Goodwin, B., Phillips, E., Mallal, S., et al. (2022). SARS-CoV-2 vaccination induces immunological T cell memory able to cross-recognize variants from Alpha to Omicron. Cell *185*, 847–859.e11. https://doi.org/10.1016/j.cell.2022.01.015.

62. Naranbhai, V., Nathan, A., Kaseke, C., Berrios, C., Khatri, A., Choi, S., Getz, M.A., Tano-Menka, R., Ofoman, O., Gayton, A., et al. (2022). T cell reactivity to the SARS-CoV-2 Omicron variant is preserved in most but not all individuals. Cell *185*, 1041–1051.e6. https://doi.org/10.1016/j.cell.2022.01.029.

63. Choi, S.J., Kim, D.-U., Noh, J.Y., Kim, S., Park, S.-H., Jeong, H.W., and Shin, E.-C. (2022). T cell epitopes in SARS-CoV-2 proteins are substantially conserved in the Omicron variant. Cell. Mol. Immunol. *19*, 447–448. https://doi.org/10.1038/s41423-022-00838-5.

64. Javanmardi, K., Chou, C.W., Terrace, C.I., Annapareddy, A., Kaoud, T.S., Guo, Q., Lutgens, J., Zorkic, H., Horton, A.P., Gardner, E.C., et al. (2021). Rapid characterization of spike variants via mammalian cell surface display. Mol. Cell *81*, 5099–5111.e8. https://doi.org/10.1016/j.molcel.2021.11.024.

65. Yan, R., Zhang, Y., Li, Y., Xia, L., Guo, Y., and Zhou, Q. (2020). Structural basis for the recognition of SARS-CoV-2by full-length human ACE2. Science *367*, 1444–1448.

66. Bwire, G.M. (2020). Coronavirus: Why Men are More Vulnerable to Covid-19 Than Women? SN Compr. Clin. Med. *2*, 874–876. https://doi.org/10.1007/s42399-020-00341-w.

67. Yuan, L., Zhu, H., Zhou, M., Ma, J., Chen, R., Chen, Y., Chen, L., Wu, K., Cai, M., Hong, J., et al. (2021). Gender associates with both susceptibility to infection and pathogenesis of SARS-CoV-2 in Syrian hamster. Signal Transduct. Target. Ther. *6*, 136. https://doi.org/10.1038/s41392-021-00552-0.

68. Channappanavar, R., Fett, C., Mack, M., Ten Eyck, P.P., Meyerholz, D.K., and Perlman, S. (2017). Sex-Based Differences in Susceptibility to Severe Acute Respiratory Syndrome Coronavirus Infection. J. Immunol. *198*, 4046–4053. https://doi.org/10.4049/jimmunol.1601896.

69. Samuel, R.M., Majd, H., Richter, M.N., Ghazizadeh, Z., Zekavat, S.M., Navickas, A., Ramirez, J.T., Asgharian, H., Simoneau, C.R., Bonser, L.R., et al. (2020). Androgen Signaling Regulates SARS-CoV-2 Receptor Levels and Is Associated with Severe COVID-19 Symptoms in Men. Cell Stem Cell *27*, 876–889.e12. https://doi.org/10.1016/j.stem.2020.11.009.

70. Wang, X., Tang, Q., Li, H., Jiang, H., Xu, J., Bergquist, R., and Qin, Z. (2023). Autoantibodies against type I interferons in COVID-19 infection: A systematic review and meta-analysis. Int. J. Infect. Dis. *130*, 147–152. https://doi.org/10.1016/j.ijid.2023.03.011.

71. Fang, Z., Monteiro, V.S., Renauer, P.A., Shang, X., Suzuki, K., Ling, X., Bai, M., Xiang, Y., Levchenko, A., Booth, C.J., et al. (2023). Polyvalent mRNA vaccination elicited potent immune response to monkeypox virus surface antigens. Cell Res. *33*, 407–410. https://doi.org/10.1038/s41422-023-00792-5.

72. Channappanavar, R., Fett, C., Zhao, J., Meyerholz, D.K., and Perlman, S. (2014). Virus-specific memory CD8 T cells provide substantial protection from lethal severe acute respiratory syndrome coronavirus infection. J. Virol. *88*, 11034–11044. https://doi.org/10.1128/JVI.01505-14.

73. Qin, J., Jeon, J.H., Xu, J., Langston, L.K., Marasini, R., Mou, S., Montoya, B., Melo-Silva, C.R., Jeon, H.J., Zhu, T., et al. (2023). Design and preclinical evaluation of a universal SARS-CoV-2 mRNA vaccine. Front. Immunol. *14*, 1126392. https://doi.org/10.3389/fimmu.2023.1126392.

74. Tai, W., Feng, S., Chai, B., Lu, S., Zhao, G., Chen, D., Yu, W., Ren, L., Shi, H., Lu, J., et al. (2023). An mRNA-based T-cell-inducing antigen strengthens COVID-19 vaccine against SARS-CoV-2 variants. Nat. Commun. *14*, 2962. https://doi.org/10.1038/s41467-023-38751-8.

75. Martinez, D.R., and Ooi, E.E. (2022). A potential silver lining of delaying the second dose. Nat. Immunol. *23*, 349–351. https://doi.org/10.1038/s41590-022-01143-z.

76. Hall, V.G., Ferreira, V.H., Wood, H., Ierullo, M., Majchrzak-Kita, B., Manguiat, K., Robinson, A., Kulasingam, V., Humar, A., and Kumar, D. (2022). Delayed-interval BNT162b2 mRNA COVID-19 vaccination enhances humoral immunity and induces robust T cell responses. Nat. Immunol. *23*, 380–385. https://doi.org/10.1038/s41590-021-01126-6.

77. Keeton, R., Tincho, M.B., Ngomti, A., Baguma, R., Benede, N., Suzuki, A., Khan, K., Cele, S., Bernstein, M., Karim, F., et al. (2022). T cell responses to SARS-CoV-2 spike cross-recognize Omicron. Nature *603*, 488–492. https://doi.org/10.1038/s41586-022-04460-3.

78. Wilhelm, A., Widera, M., Grikscheit, K., Toptan, T., Schenk, B., Pallas, C., Metzler, M., Kohmer, N., Hoehl, S., Marschalek, R., et al. (2022). Limited neutralisation of the SARS-CoV-2 Omicron subvariants BA.1 and BA.2 by convalescent and vaccine serum and monoclonal antibodies. EBioMedicine *82*, 104158. https://doi.org/10.1016/j.ebiom.2022.104158.

79. VanBlargan, L.A., Errico, J.M., Halfmann, P.J., Zost, S.J., Crowe, J.E., Jr., Purcell, L.A., Kawaoka, Y., Corti, D., Fremont, D.H., and Diamond, M.S. (2022). An infectious SARS-CoV-2 B.1.1.529 Omicron virus escapes neutralization by therapeutic monoclonal antibodies. Nat. Med. *28*, 490–495. https://doi.org/10.1038/s41591-021-01678-y.

80. Wang, C.Y., Peng, W.J., Kuo, B.S., Ho, Y.H., Wang, M.S., Yang, Y.T., Chang, P.Y., Shen, Y.H., and Hwang, K.P. (2023). Toward a pan-SARS-CoV-2 vaccine targeting conserved epitopes on spike and non-spike proteins for potent, broad and durable immune responses. Plos Pathog. *19*, e1010870. https://doi.org/10.1371/journal.ppat.1010870.

81. Zhang, Z., Mateus, J., Coelho, C.H., Dan, J.M., Moderbacher, C.R., Gálvez, R.I., Cortes, F.H., Grifoni, A., Tarke, A., Chang, J., et al. (2022). Humoral and cellular immune memory to four COVID-19 vaccines. Cell *185*, 2434–2451.e17. https://doi.org/10.1016/j.cell.2022.05.022.

82. Freyn, A.W., Ramos da Silva, J., Rosado, V.C., Bliss, C.M., Pine, M., Mui, B.L., Tam, Y.K., Madden, T.D., de Souza Ferreira, L.C., Weissman, D., et al. (2020). A Multi-Targeting, Nucleoside-Modified mRNA Influenza Virus Vaccine Provides Broad Protection in Mice. Mol. Ther. *28*, 1569–1584. https://doi.org/10.1016/j.ymthe.2020.04.018.

83. Li, D., Martinez, D.R., Schäfer, A., Chen, H., Barr, M., Sutherland, L.L., Lee, E., Parks, R., Mielke, D., Edwards, W., et al. (2022). Breadth of SARS-CoV-2 neutralization and protection induced by a nanoparticle vaccine. Nat. Commun. *13*, 6309. https://doi.org/10.1038/s41467-022-33985-4.

84. Maier, M.A., Jayaraman, M., Matsuda, S., Liu, J., Barros, S., Querbes, W., Tam, Y.K., Ansell, S.M., Kumar, V., Qin, J., et al. (2013). Biodegradable lipids enabling rapidly eliminated lipid nanoparticles for systemic delivery of RNAi therapeutics. Mol. Ther. *21*, 1570–1578. https://doi.org/10.1038/mt.2013.124.

85. Jayaraman, M., Ansell, S.M., Mui, B.L., Tam, Y.K., Chen, J., Du, X., Butler, D., Eltepu, L., Matsuda, S., Narayanannair, J.K., et al. (2012). Maximizing the potency of siRNA lipid nanoparticles for hepatic gene silencing *in vivo*. Angew. Chem. Int. Ed. Engl. *51*, 8529–8533. https://doi.org/10.1002/anie.201203263.

86. Remakus, S., Rubio, D., Lev, A., Ma, X., Fang, M., Xu, R.H., and Sigal, L.J. (2013). Memory CD8(+) T cells can outsource IFN-gamma production but not cytolytic killing for antiviral protection. Cell Host Microbe *13*, 546–557. https://doi.org/10.1016/j.chom.2013.04.004.

87. Ábrahám, E., Bajusz, C., Marton, A., Borics, A., Mdluli, T., Pardi, N., and Lipinszki, Z. (2024). Expression and purification of the receptor-binding domain of SARS-CoV-2 spike protein in mammalian cells for immunological assays. FEBS Open Bio *14*, 380–389. https://doi.org/10.1002/2211-5463.13754.

88. Alameh, M.G., Tombácz, I., Bettini, E., Lederer, K., Sittplangkoon, C., Wilmore, J.R., Gaudette, B.T., Soliman, O.Y., Pine, M., Hicks, P., et al. (2021). Lipid nanoparticles enhance the efficacy of mRNA and protein subunit vaccines by inducing robust T follicular helper cell and humoral responses. Immunity *54*, 2877–2892.e7. https://doi.org/10.1016/j.immuni.2021.11.001.